TECHNICAL REPORT
NATICK/TR-05/010

AD_____

BIOLOGICALLY-INSPIRED MICRO-ROBOTS:

Volume 1, Robots Based On Crickets

by
Roger Quinn
Roy Ritzmann
Stephen Phillips
Randall Beer
Steven Garverick
and
Matthew Birch

Case Western Reserve University
Cleveland, OH 44106-7222

May 2005

Final Report
June 1998 – September 2002

Prepared for
U.S. Army Research, Development and Engineering Command
Natick Soldier Center
Natick, Massachusetts 01760-5020

DISCLAIMERS

The findings contained in this report are not to be construed as an official Department of the Army position unless so designated by other authorized documents.

Citation of trade names in this report does not constitute an official endorsement or approval of the use of such items.

DESTRUCTION NOTICE

For Classified Documents:

Follow the procedures in DoD 5200.22-M, Industrial Security Manual, Section II-19 or DoD 5200.1-R, Information Security Program Regulation, Chapter IX.

For Unclassified/Limited Distribution Documents:

Destroy by any method that prevents disclosure of contents or reconstruction of the document.

REPORT DOCUMENTATION PAGE

Form Approved
OMB No. 0704-0188

1. REPORT DATE *(DD-MM-YYYY)*	2. REPORT TYPE	3. DATES COVERED *(From - To)*
19-05-2005	Final Report	June 1998 - September 2002

4. TITLE AND SUBTITLE
BIOLOGICALLY-INSPIRED MICRO-ROBOTS:
Volume 1, Robots Based On Crickets

5a. CONTRACT NUMBER
C-DAAN02-98-C-4027

5b. GRANT NUMBER

5c. PROGRAM ELEMENT NUMBER

6. AUTHOR(S)
Roger Quinn, Roy Ritzmann, Stephen Phillips, Randall Beer, Steven Garverick, and Matthew Birch

5d. PROJECT NUMBER

5e. TASK NUMBER

5f. WORK UNIT NUMBER

7. PERFORMING ORGANIZATION NAME(S) AND ADDRESS(ES)
Case Western Reserve University
Mechanical Engineering Dept.
10900 Euclid Avenue
Cleveland, OH 44106-7222

8. PERFORMING ORGANIZATION REPORT NUMBER

9. SPONSORING/MONITORING AGENCY NAME(S) AND ADDRESS(ES)
Sponsor: Defense Advanced Research Projects Agency (DARPA)
Microsystems Technology Office (Elana Ethridge)
3701 North Fairfax Drive
Arlington, VA 22203-1714

10. SPONSOR/MONITOR'S ACRONYM(S)

11. SPONSOR/MONITOR'S REPORT NUMBER(S)
NATICK/TR-05/010

12. DISTRIBUTION/AVAILABILITY STATEMENT
Approved for public release; distribution is unlimited.

13. SUPPLEMENTARY NOTES
Monitor: US Army Research, Development & Engineering Command, Natick Soldier Center, ATTN: AMSRD-NSC-SS-MA (T. Gilroy), Kansas Street, Natick, MA 01760-5020

14. ABSTRACT
This is one of three reports on the study of micro-robots. This document describes the design and construction of a series of small robotic vehicles. The designs incorporate biological inspiration from the cricket. The goal is a micro autonomous legged robot capable of traveling over a variety of terrains. The development of many components needed to build the robot, such as micro-McKibben artificial muscles, micro compressors, and MEMS (micro-electro-mechanical systems) - fabricated valves is also discussed. These components were first used in the design and construction of several prototype sub-systems such as a prototype leg and a simple non-autonomous hybrid vehicle that tests individual components before use in the fully integrated vehicles. From these prototypes two versions of an autonomous vehicle that use a combination of legs and wheels to locomote were developed. Two wheels support the front of the vehicles and two rear legs propel them. The valves distribute air, supplied by the compressor, from the plenum to the actuators on the rear legs. A six-legged non-autonomous vehicle was designed, constructed, tested, and demonstrated to walk in a tripod gait. A second report (NATICK/TR-05/011) focuses on the investigation of a micro-joint angle sensor using MEMS Cilia, and a third report (NATICK/TR-05/012) examines micro-robots on abstracted biological principles.

15. SUBJECT TERMS

MICROROBOT	BIOLOGICALLY INSPIRED	MICRO ACTUATORS	LOCOMOTION
CRICKETS	LEGGED VEHICLES	AUTONOMOUS VEHICLES	MICROVALVES
ROBOTS	DESIGN(ENGINEERING)	TERRAIN	GAIT
ROBOTIC VEHICLES	TEST AND EVALUATION	MEMS (MICRO-ELECTRO-MECHANICAL SYSTEMS)	

16. SECURITY CLASSIFICATION OF:			17. LIMITATION OF ABSTRACT	18. NUMBER OF PAGES	19a. NAME OF RESPONSIBLE PERSON
a. REPORT	b. ABSTRACT	c. THIS PAGE			Thomas Gilroy
U	U	U	SAR	86	19b. TELEPHONE NUMBER *(Include area code)* 508-233-5855

TABLE OF CONTENTS

CONTENTS (Cont'd)

LIST OF FIGURES

FIGURES (Cont'd)

FIGURES (Cont'd)

FIGURES (Cont'd)

PREFACE

This report outlines the research undertaken by Case Western Reserve University, Cleveland, OH, and Carnegie Mellon University, Pittsburgh, PA to develop micro-robots and the components needed to fabricate those micro-robots. Two types of robots, each 3 inches long, resulted from this work along with several important components. This report is presented in three volumes: The first volume describes the development of a robot based upon a cricket; the second volume describes the development of MEMS joint angle sensors based upon cilia; the third volume describes another type of robot that can run faster than any other legged vehicle of its size, run over relatively large obstacles, and operate for several hours without a change of batteries. The purpose of this report is to communicate the design, implementation and evaluation of these unique micro-robots and their essential components. The project was completed during the period June 1998 to September 2002 under contract number C-DAAN02-98-C-4027, under the direction of U.S. Army Research, Development and Engineering Command, Natick Soldier Center, Natick, MA, and sponsorship of the Defense Advanced Research Projects Agency (DARPA), Arlington, VA.

This report is one of a series of three. The references for the other reports are:

Fedder, Gary K., and de Rosset, Lauren Elizabeth. (2005) *Biologically-Inspired Micro-Robots: Vol.2, Investigation of a Micro-Joint Angle Sensor Using MEMS Cilia,* Technical Report, (NATICK/TR-05/011), U.S. Army Research, Development and Engineering Command (RDECOM), Natick Soldier Center, Natick, MA 01760.

Quinn, R., Ritzmann, R., Morrey, J., and Horchler., A. (2005) *Biologically-Inspired Micro-Robots: Vol. 3, Micro-Robot Based on Abstracted Biological Principles,* Technical Report, (NATICK/TR-05/012), U.S. Army Research, Development and Engineering Command (RDECOM), Natick Soldier Center, Natick, MA 01760.

BIOLOGICALLY INSPIRED MICRO-ROBOTS

Volume 1: Robots Based on Crickets

SUMMARY

This is the first of three volumes describing the work performed in the Biologically Inspired Micro-Robots project. The overall goal of the project was to develop legged vehicles that can run and jump and that can fit in a 2-inch cube. Many technologies needed to be advanced in order for this project to succeed. In this volume the development of micro actuators, MEMS valves and small compressors are described along with the design of legged vehicles that use these new components. Volume 2 will describe the development of joint angle sensors for micro legged robots using MEMS fabrication processes. Volume 3 will describe the development of micro robots that can run and jump based upon more abstracted biological principles.

This report (Volume 1) describes the design and construction of a series of small robotic vehicles. The designs incorporate biological inspiration from the cricket. The ultimate goal is a micro autonomous legged robot capable of traveling over a variety of terrains. The development of many components needed to build such a robot, such as micro braided pneumatic actuators, a micro compressor, MEMS fabricated valves, and MEMS sensors is also discussed. These components were first used in the design and construction of several prototype sub-systems such as a prototype leg and a simple nonautonomous hybrid vehicle that tests individual components before use in the fully integrated vehicles. From these prototypes two versions of an autonomous vehicle that use a combination of legs and wheels to locomote were developed. Finally, a six-legged non-autonomous vehicle was designed, constructed and tested.

1. INTRODUCTION

1.1 Motivation

The Defense Advanced Research Projects Agency's (DARPA) Distributed Robotics Program's mission statement (quoted in part below) provided motivation for the project team.

"The DARPA Distributed Robotics Program seeks to develop revolutionary approaches to extremely small robots, reconfigurable robots, systems of robots, biologically-inspired designs, innovative methods of robot control including innovative interfaces, and methods of implementing pooled capabilities and/or layered intelligence. The program focus is upon individual robots that are less than 5 centimeters in any dimension; however, novel methods of long-range deployment may involve larger transport vessels. Potential applications for such robots or systems of robots include surveillance, reconnaissance, path finding, deception, weapon delivery, transporting artifacts, and small scale actuation. The development of micro and miniature robots offers a variety of technical challenges. Chief among these are mechanisms of locomotion for low-mass devices, integration of low-power electronic control and payloads, energy sources, and human robot control. Finally, robots can either be fully controlled by humans, semi-autonomously controlled, or operate autonomously. Control architectures and human interface technology are needed for successful mission accomplishment."

1.2 Purpose

The purpose of the project was to develop an autonomous micro-robot. A possible mission for this robot is to be the eyes and ears of war fighters in urban combat. The robot must be able to move in various terrains commonly encountered while navigating an urban combat environment. The robot also must be able to carry a small payload of sensors and communications equipment.

Mission times were to be on the order of minutes, if deployed by warfighters, or hours or possibly a day or two if delivered to the combat zone ahead of time by some other means. One of the driving ideas behind the overall Distributed Robotics Program is that the robots can be relatively inexpensive and be deployable in large groups. This has a twofold purpose. First, it provides redundancy. The robots are small for ease of deployment and stealth, but their small size is also their weakness. Even a robust robot of only 2 cubic inches may have difficulty navigating an unknown terrain. Also, since discovery by the adversary may terminate the robot's mission, more than one robot helps to insure the mission is completed successfully.

To accomplish the overall mission, many technologies had to be developed: the robot itself, the sensors it would carry, the equipment it would use to communicate with the other robots in the swarm and their relay of gathered information back to the commanders and soldiers that would need it. Swarm behaviors also need to be developed to take advantage of a multitude of small robots.

Our goal was to develop a small mobile robotic platform that could carry the required sensors and communication equipment. We proposed a micro-robot that could walk through a variety of

terrain and jump over obstacles such as standard stairs. Crickets both walk and jump well. Therefore, we proposed to develop a cricket inspired robot that could both walk and jump.

This report describes the development of the robot from the initial concept to a prototype test leg and stand-alone compressor, to an autonomous wheel-leg hybrid vehicle, and finally to a six-legged mobile platform. The required technologies and components to reach this point are also described.

2. BACKGROUND

2.1 Previous Work in the CWRU Biorobotics Lab

The Biorobotics Lab at Case Western Reserve University (CWRU) has focused its attention on building mobile robots based on design and control principles learned from walking animals. Much of our research is based on studies of insect locomotion. The robots are also useful models for the biologists and a beneficial exchange of ideas and support has been established. The Biorobotics Lab was started in 1989 with research involving a line of progressively more complex and capable hexapod robots. This work was supported by the Office of Naval Research.

Robot I (see Figure 1) was the first in the series of hexapods [15] and it was built to test a neural network gait controller [3]. It used six identical two degree-of-freedom (DOF) legs. Each leg included a rotational and telescoping DOF. The robot and controller successfully demonstrated insect-like gaits.

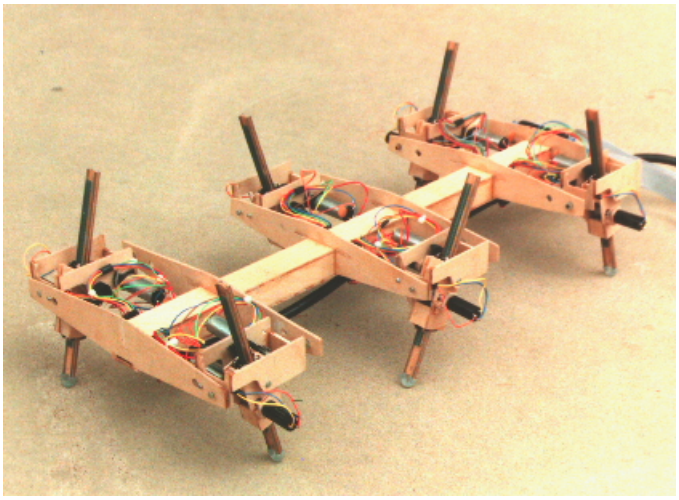

Figure 1. Robot I

Continuing on the promising success of Robot I, Robot II (see Figure 2) was constructed. Robot II again used six identical legs but the legs used 3 revolute joints that permitted a sprawled insect-like posture. Along with a gait controller similar to the one developed with Robot I, a series of reflexes was added to give the robot the ability to locomote over much more

complicated and difficult terrain. So combining a more capable robot and controller Robot II was a very successful robot and able to locomote omnidirectionally in a variety of gaits over a variety of terrain.

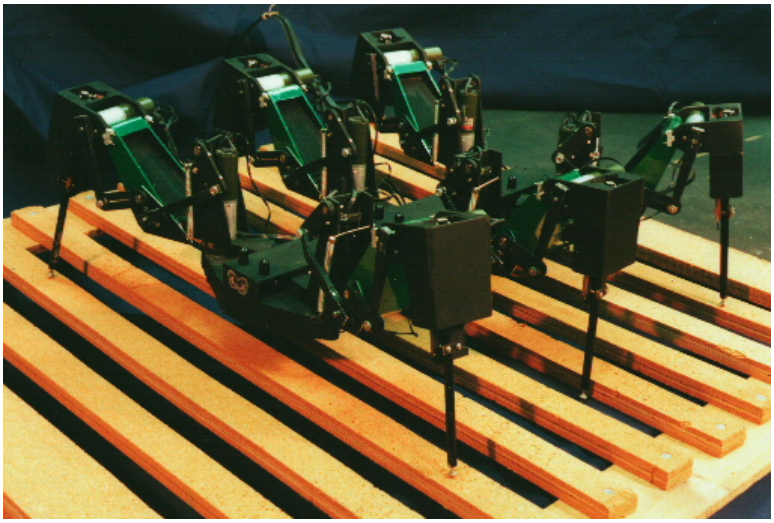

Figure 2. Robot II

Next in the line of hexapod robots was Robot III [2] (Figure 3). Where Robot I and Robot II used gear motors, Robot III uses valves and air cylinders to actuate its joints. Robot III also used a much more biologically-inspired design for the structure of the robot. Its kinematics were a simplification of the *Blaberus discoidalis* cockroach. Although the number of degrees of freedom was reduced from those in the cockroach, the leg proportion and locomotive function is an accurate reproduction of the cockroach. The robot is approximately 17 times the size of the insect, making the robot about 30 inches long. The pneumatic actuation enabled the robot to be stronger than its predecessors, but pneumatic cylinders proved to be more difficult to control [25] than the gear motors.

The next robot in the series is Robot IV (see Figure 4). Similar in kinematic arrangement to Robot III, based on the cockroach, but instead of using traditional pneumatic cylinders it uses braided pneumatic actuators. The robot is even lighter than Robot III because of this change of actuation. Work on devising a controller for this robot is ongoing in the Biorobotics Lab.

2.2 Small Robots

There have been many small robots built for a variety of missions, but a majority of them are for behavioral and navigation strategy research and hence, they are simple, wheeled robots with very limited mobility. Robots, like the commercially-available K-Team's Khepera robots, have only two small drive wheels and one or more idler wheels [21]. They can function on only very smooth, flat surfaces. Small robots with wheels typically turn by driving the contralateral wheels

separately much like a tracked vehicle does. At this scale, tracks appear to provide minimal advantage over wheels but other research groups like one at Carnegie Mellon University have used them on their millibots [4].

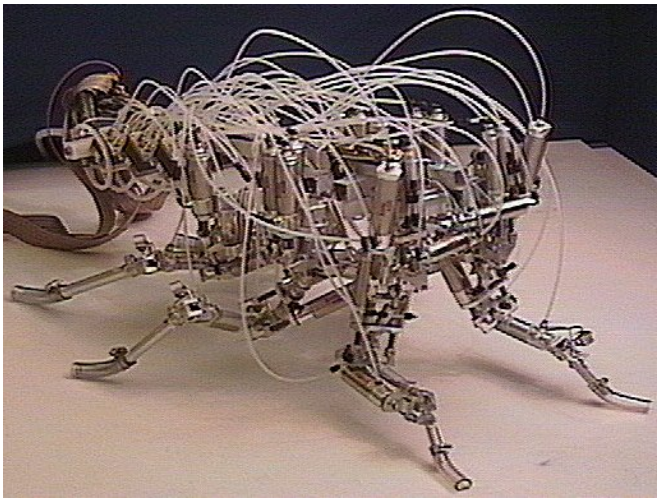

Figure 3. Robot III

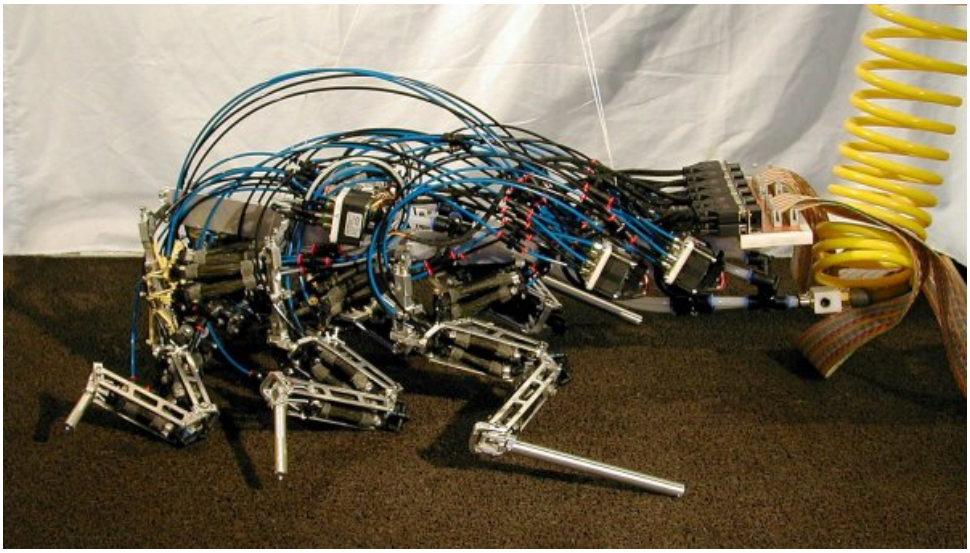

Figure 4. Robot IV

There are a few robots at this scale that are capable of rough terrain. Scout, a robot from another member of the DARPA Distributed Robotics Program, can roll on relatively large wheels for its size and some versions of it have the ability to jump up a stair or use expanding wheels to overcome larger obstacles [13].

Most small robots use wheels for locomotion but some use tracks [7]. This modestly improves their mobility, but they lack the room for the complexity of modern track suspension and therefore their performance increase is not significant. It seems that this choice offers better traction than wheels, but without the suspension, the height of obstacles they can climb is only marginally higher than that for a wheeled robot of a similar scale.

Robots like the Alice series were capable of a variety of missions but their locomotion was limited because of their very small size [6]. These robots used wheels that were relatively large compared to the size of the robot.

Piezoelectric actuation shows some promise for small robots but because of the high voltage and very small excursions, they are not practical on rough terrain micro robots. Piezoelectric actuators also function more efficiently at high frequency and this adds another level of complexity to convert the high frequency small amplitude motion into slower, controllable, larger range motion.

Fukui [16] has produced a micro robot that uses the high frequency efficiency of the piezoelectric actuators for a unique locomotion. It inch worms itself along with a tripod stance, but since the robot is essentially shuffling along it is limited to flat, smooth surfaces.

Another group of specialized robots that use piezoelectric actuators are the pipe robots developed at Shanghai University, China [23]. The university developed two robots: one with a gripper and one with a camera, that each uses piezoelectric actuation to inch along in a pipe. They were developed for very specific terrain that allows them to take advantage of the small strain, high-frequency motion of the piezoelectric actuators.

Another robot in development that uses piezoelectric actuation is a micro robot fly at UC Berkeley. It uses piezoelectric actuators in an application that promises to create a more capable and flexible robot that will not be as limited by it surroundings. The piezoelectric actuators fit the application well with their high frequency efficiency. They use the actuators to flap a pair of small wings to generate lift and fly; the wingspan is 10-25mm wide [28]. A pair of four-bar mechanisms is used to actuate each wing to give it the necessary movement for not only flapping but also rotation for flight control.

2.3 Hybrid Wheel-Leg Vehicles

The hybrid wheel-leg robot or “cricket cart” described in this report is not completely unique. There are many examples of similar robots that came before or concurrently with our vehicle. For example, an autonomous robot named Autopod 0.33 [10] has a configuration that is similar to the cricket cart but it runs in the opposite direction. Our cricket cart has the legs in the back and the wheels in the front. The Autopod 0.33 has the wheels in the back and the legs in front. It does resemble the cricket cart; except that it is about 5 feet tall and 6 feet long. It uses large McKibben artificial muscles to power its legs and has an onboard compressor and controller.

The robot Wheeleg [24] is a smaller hybrid wheel-leg vehicle. It stands 26 inches tall and is about three and half feet long, but it is still much larger than our vehicle. It also has its legs in the front, like Autopod 0.33. Where Autopod uses three DOF legs, driven by McKibben Actuators, the Wheeleg robot uses traditional air cylinders and has only two DOF legs.

There have been other variations of the hybrid wheel-leg robot. Roll-walker [14] has four legs and the wheels are mounted on the ends of the legs. This makes for a very different type of locomotion. In the case of Roller-walker, the robot transforms from walker to skater. The wheels can be rotated orthogonal to their rolling axis and used as feet, walking on the sides of the wheels or turning to allow them to roll. They are passive and the robot skates much as a human skates, but on all fours.

Other hybrid wheel-leg robots have driven wheels and the legs act like an active suspension that can lift the wheels over obstacles. However, most of the forward locomotion comes from the drive motors on the wheels. Leg-wheel [1] is just such a robot. It uses electric motors to drive the legs and the wheels. There are two large wheels on one DOF legs in the rear and two small drive wheels on the end of the three DOF legs in the front. This robot functions in three modes: legged mode where the front legs pull the robot along, hybrid mode where the wheels drive and the legs help conform and climb over the obstacles, and finally the wheeled mode where the legs are locked out and the robot simply drives along on its wheels.

2.4 Miniature Six-Legged Robots

Sprawlita [9] is a six-legged robot that uses a hybrid actuator system that combines servo motors and air cylinders for leg actuation. Each leg has two DOF, with servos rotating the body femur joint and air cylinders telescoping the tibia/tarsus. The robot has passive compliance built into its femur segment. It is very energetic during locomotion but is unlikely to be able to maintain that energetic behavior in an autonomous mode. When this report was written, the robot used an off-board air compressor that provided 90 psi air.

2.5 Cricket Biology

Biologists have been interested in crickets for many reasons. Cricket sensory, neuromuscular, neuroendocrine, and central nervous system structures and mechanisms have all been studied [17]. The complex behaviors of the cricket have been investigated both in the lab and in the field. As a non-aggressive insect, crickets cannot sting, and this makes lab work more pleasant. The cricket's song is of special interest because of the accessibility the biologists have to analysis tools and its connection to many interesting cricket behaviors [33].

For this project we chose to study the cricket because of its combination of locomotion methods. Because the cricket both runs and jumps well it has a great amount of locomotion flexibility. The cricket is not as accomplished at running and climbing as the *Blaberus discoidalis* cockroach [34], but the cricket is still a capable runner. It also is not as powerful a jumper as the locust and grasshopper [31], but it can jump well. The cricket's compromise between running and jumping make it a good model for a small mobile robot.

One of the essential features that make the cricket a powerful jumper is its pair of large, strong rear legs [18], [32]; its rear legs are about 2.5 times larger than its front or middle legs. We also learned that the cricket's front legs are important for running and jumping and are well designed

for these functions [22]. For example, the front and middle legs pitch the body up before a jump. Therefore, because of the locomotion flexibility found in the cricket, we chose it as the basis for the inspiration for the micro robots that are discussed in this report.

3. SYSTEM OVERVIEW

For the robot that was the goal of this work, many individual systems needed to be developed. Most of these systems will be explained in greater detail in later sections, but they are introduced here in terms of a system overview and robot design concept.

The goal of the project was to develop a small robot that could navigate a variety of terrains. It was to be a legged robot designed using inspiration from crickets.

It was necessary to make many decisions in the conceptual design stage. The most significant of these was our decision to use a pneumatic power system. This enabled us to take advantage of the many beneficial features that McKibben actuators have for a legged robot. Pneumatic actuation at this scale can provide a powerful and efficient method of producing locomotive forces. Other methods were considered. We considered creating a micro version of Robot II mentioned in the background. This would be a robot using small gear motors to actuate each joint. The use of piezoelectric actuators was also examined, but they are most efficient at frequencies too high for this application.

A conceptual drawing of a six-legged micro robot is shown in Figure 5. The robot's onboard power plant is a battery powered motor-compressor system. The compressor delivers the air that activates the actuators that propel the robot. Based upon scaling studies we determined that the compressor must be capable of 20psi at a flow rate of 0.1 liters per minute (LPM). Since commercially-available compressors of this size are not available, one was designed and constructed.

The actuators for the robot needed to be developed for the project since no commercially-available braided pneumatic actuators were available at this scale. Braided pneumatic actuators (also known as McKibben artificial muscles or Rubbertuators™) have been used for many years, but construction of actuators as small as were needed had not been done before. Fabrication methods were developed to produce the small actuators for the project.

Valves were needed to distribute compressed air to the actuators and those were also not commercially available. We developed Micro-Electro-Mechanical Systems (MEMS) fabricated micro valves [29] for this purpose.

The general structure and legs for the robot were also designed. Although the cricket inspired the design, we did not attempt to directly copy the cricket. Instead, the animal was used as an inspiration for locomotion principles that guided the designs.

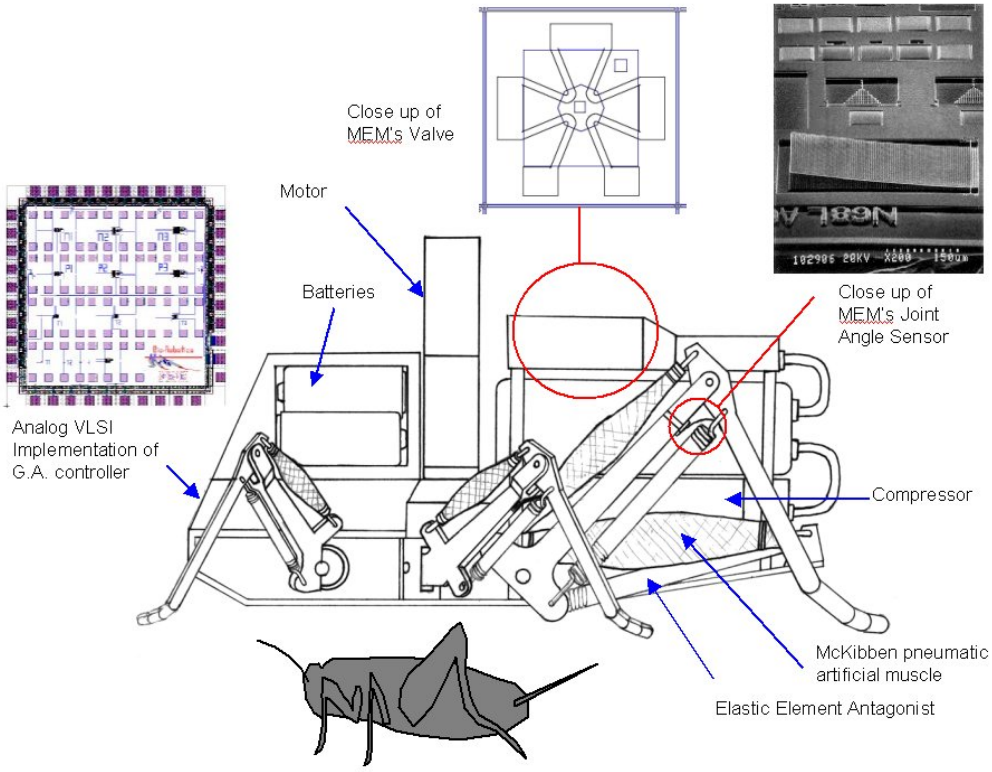

Figure 5. Early Concept Drawing of the Cricket Robot

3.1 Tools Used in Design and Construction

There were many engineering tools used in the design and fabrication process. The robot was designed in AutoDesk's Mechanical Desktop. This software is a 3-D parametric drawing package that allows one to design parts and assemble them so that the user can check things like interference, kinematic compliance and estimate masses and volumes of the parts and assembly.

Several spreadsheets in Microsoft Excel, as well as hand calculations, were used. These spreadsheets performed calculations such as kinematic analysis of data collected from the high speed video of crickets walking as well as calculating the design space of the compressor and analyzing the compressor flow rates to estimate how changes in that design space would change the performance of the compressor.

A specially written dynamic simulation was also used in the design. A C++ simulation of the two-legged cricket cart was developed for design and controller development.

The majority of the machined parts for the cricket robots were made on a pair of Rolland CNC desktop mills (see Figure 6). Control codes for these machines were exported from Mechanical Desktop. Along with the two desktop CNC mills, a manually operated mill and lathe were also used for some operations. The rest of the construction was done with a variety of small hand tools such as scalpels, jeweler's files, snap saws, hemostats, dissection tweezers and others (see

Figure 7). Some hand tools such as small center punches and a very small brass hammer were made for the project. A Dremel drill press was used often for the shaping of the small metallic parts like the brass crank for the compressor and stainless steel tubing. Due to the Dremel's lack of low speed torque it was not used to drill many of the small holes required in the construction of the robot's parts. Low speed drilling is recommended for plastic parts to avoid thermal deformations. Instead, a Maxon gear motor with a small drill chuck attached was used for much of the drilling.

Figure 6. Left: PCN-3100. Right: PCN 2500

Figure 7. Hand Tools

Matrix valves (see Figure 8) and their amplifiers were used for control of the non-autonomous versions of various components and robots throughout the project.

Figure 8. Matrix Valve Block Array

4. MACHINING

4.1 Machines

General construction and machining of all parts -- with the exception of the valves -- were done in-house. The majority of the parts that were machined were made from Delrin, which is easily machined and is very tough. Its shortcomings are that it has a slightly lower than desired modulus, and it is denser than desired. However, the machinability of this material outweighs its shortcomings for construction of prototypes.

The parts were machined on one of two Roland CNC Mills shown in Figure 9. The two models used were the Roland PNC-2500 and the PNC-3100. The PNC-2500 has a smaller workspace of about 8 inches x 6 inches x 5 inches and with the tooling available, it can spin tools 1/8 inch and smaller. Most parts were machined with 1/8 inch, 1/16 inch, or 1/32 inch diameter end mills. There were a few parts that had features that required machining with a 1/64 inch diameter end mill. Use of end mills this small took advantage of the ability of the PNC-2500 to spin tools at up to 12,000 RPM. This high tool speed is desirable with the smaller tools (1/32 inch and smaller) to get smooth surface finish. The PNC-3100 runs at 8,000 rpm but has more spindle horsepower and a larger work area of 10 inches x 8 inches x 8 inches. Operation of both machines was very similar, using the same software and many of the same settings.

Figure 9. Left: PNC-3100, Right: PNC-2500

4.2 Software

All parts were designed in AutoDesk's Mechanical Desktop (although Pro-E or any other 3D modeling software capable of .stl (Stereolithography files) file format output would be usable). A screen shot with a rendering of the Cricket Cart II is seen in the above Figure 10. The finished parts, while still in Mechanical Desktop, were mounted in a sprue (see Figure 11), much like what one would find in a model car or airplane kit, and this assembly is output as an .stl file. The .stl file is then opened in a Roland program called Modela that performs the tool calculations. A screen shot of the program can be seen in Figure 12. The input parameters include tool size and shape, part scale, part orientation, and a variety of tool feed and spindle speed settings. The program did all the tool path calculations and fed this code to the machine. Feed rates were all determined starting with very conservative parameters preprogrammed into the software from Roland and increased in increments after some experience with the machines to reduce machine times and increase the productivity of the machines.

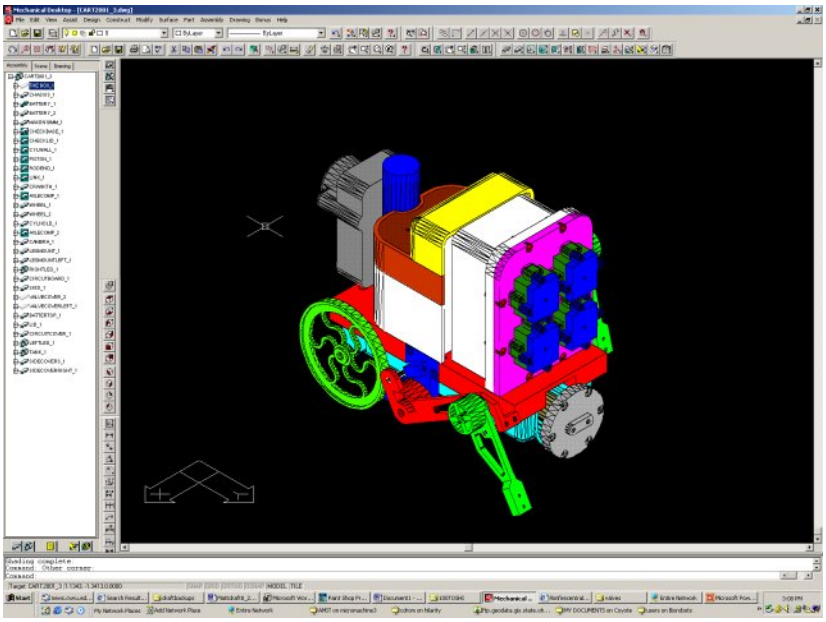

Figure 10. Screen Shot of Mechanical Desktop Model of Cricket Cart Robot

The unique part of our process was the setup developed for turning the parts over so double-sided parts could be machined. A hole was drilled through the lower left corner of the blank. This acted as a reference point for when the part was flipped over. Alignment of the hole was made to again put the center of this hole at 0,0 machine coordinates. A second copy of the .stl files, in a different orientation, was required to achieve proper orientation of the parts for the second side.

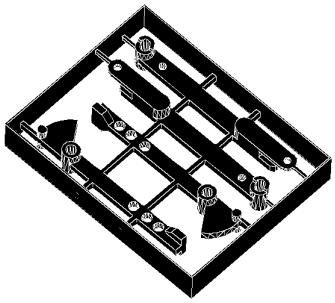

Figure 11. Example of Parts Mounted in a Frame Ready for Machining.

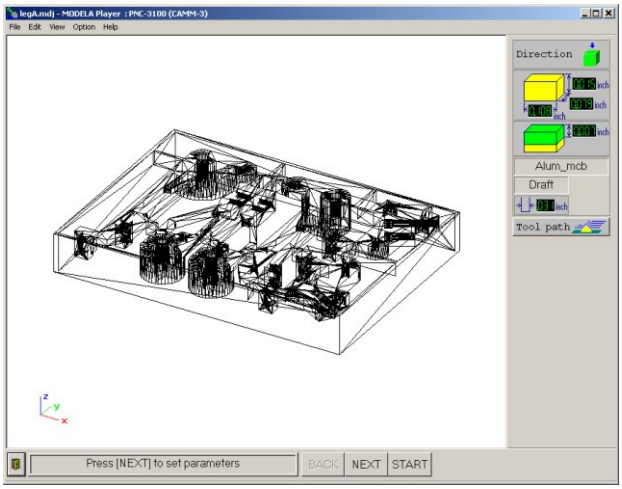

Figure 12. Screen Shot of Modela Player with the Femur and Tibia Parts for Cricket Cart II Loaded

4.3 Fasteners and Other Components

Other materials were used in the construction of these various robots. The following fasteners, some of which can be seen in Figure 13, were used to assemble the robot, 00-90, 0-80, and 1-72 screws of various types, binding head screws, fillister screws, and cap screws (0-80 and 1-72

only). Because of the machinability of Delrin, many holes were hand tapped for all the threads involved. Building the compressor required tapping holes in brass and aluminum. This was needed for the 0-80 and 1-72 cap screws and was achieved using standard hand taps.

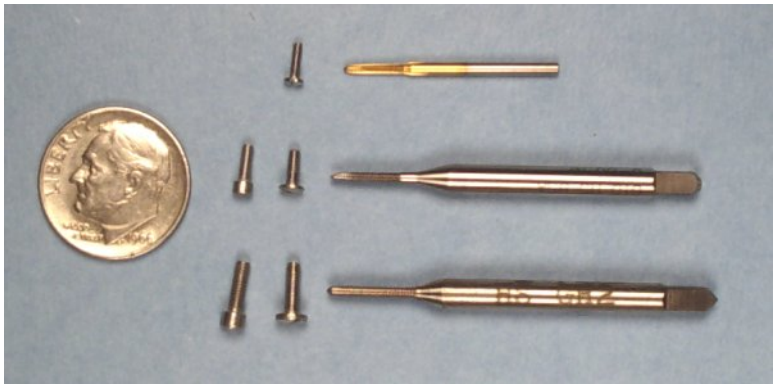

Figure 13. Top to Bottom: 00-90 Screw, 00-90 Tap; 0-80 Cap Screw, 0-80 Screw, 0-80 Tap; 1-72 Cap Screw, 1-72 Screw, 1-72 Tap; US Dime for scale

Extensive use of hypodermic needle tubing was used for air fittings and axles. A 17-gage tubing was used for all air fittings. This was determined from a compromise in hose material. Light yet flexible tubing was needed, but if the tubing were too small in ID, the head losses would be unacceptable. After some experimentation with types and sizes, it was determined to use Silactic® laboratory tubing made by Dow Corning and is made of silicone rubber. It has an ID of 0.040 inches and an OD of 0.085 inches. This size requires that 17-gage tubing be used to make an adequate press fitting for connecting the tubing. The stainless steel tubing was also press-fit into any Delrin parts that needed fittings, such as the valve packages and pressure manifolds, with an approximately 0.003 inch interference fit. An example of fitting pressed into Delrin and hose connection can be seen in Figure 14. This press fit was fairly leak-proof and if a leak did develop, it was quickly sealed with Super Glue.

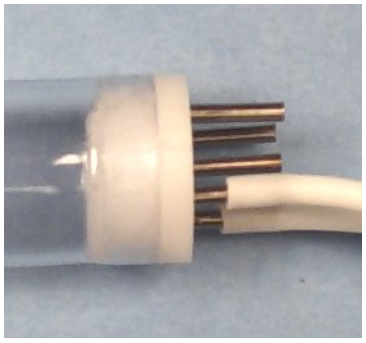

Figure 14. Picture of End of Cricket Cart I Pressure Manifold Fittings with and without Tubing.

Rotating joints were made using either 15- or 13- gage hypodermic tubing. This was chosen because 15- and 13- gage hypodermic tubing fits closely over 0-80 and 1-72 screws, respectively. An example of this construction can be seen in Figure 15. This made assembly and disassembly of the joints easy and yet strong.

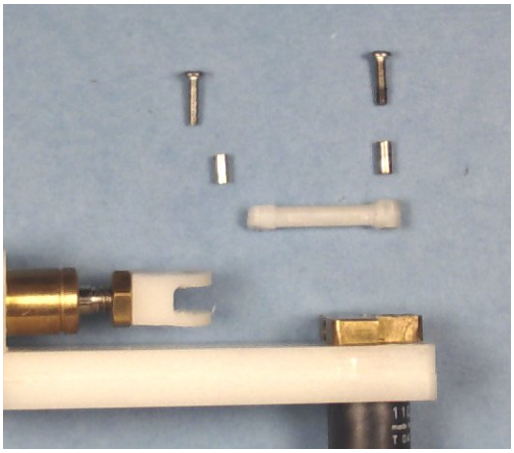

Figure 15. Exploded view of Maxon Compressor Linkage Showing Axle Tubing and Screws

Other materials used were 0.005 -0.010 inch thick spring steel to make the rear leg tarsus (see Figure 16). Brass shim stock was used as strapping material to assemble much of the second-generation cricket cart's various covers (see Figure 17).

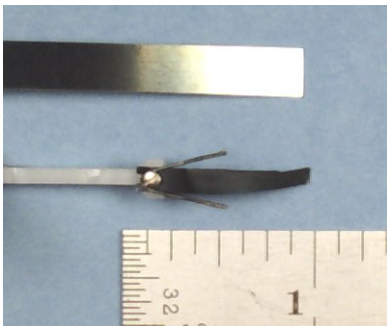

Figure 16. Top: Spring Steel Stock, Bottom: Spring Steel Tarsus and Spines from Cricket Cart I

Early actuator tendons used monofilament line but this proved to be too stiff and in the second generation cricket cart and the six-legged robot, silk suture was used because of its high tensile strength and very low bending stiffness.

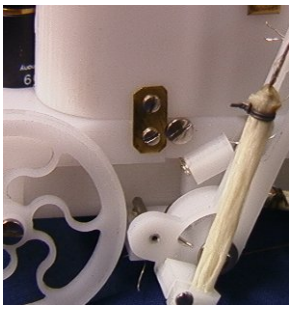

Figure 17. Brass Strap in Center of Image Holds the Upper Cover to the Chassis of Cricket Cart II

5. ACTUATORS

5.1 Introduction

For this project, braided pneumatic actuators were used throughout for activation of leg joints. These actuators were chosen for several reasons. First, we had decided to use a pneumatic power plant as explained earlier in the Section 3. This narrowed the choice to some type of pneumatic actuator, for example air cylinders or braided pneumatic actuators. Other common pneumatic actuators like air turbines are not directly useful because their high speeds are not suitable for activating robotic legs. We had to choose between air cylinders and braided pneumatic actuators, which each have advantages and disadvantages.

Air cylinders have several advantages. They can be made double-acting, allowing one actuator to actuate a joint in both directions. Air cylinders are also dimensionally well defined. They have attachment points that are easy to define and are consistent from actuator to actuator, thus making the mounting of the actuator to the robots structure more direct and at higher tolerances. They also are widely used and there exists a great wealth of knowledge about them and so the commercially available cylinders are both reliable and inexpensive. Also, because of their rigid construction and function they rarely fail in such a way as to destroy themselves. Failure usually happens in ways that reduce efficiency of an actuator but without disabling it.

Braided pneumatic actuators are also known as McKibben artificial muscles [8], [20] or Rubbertuators [27], but they will be referred to as braided pneumatic actuator (BPA) for this report. They were patented in 1957 but have not been used extensively. The principal of operation is simple. Enclose a tubular, inflatable bladder within a tubular counter spiraling interwoven inextensible fiber mesh, seal one end and port the other for high pressure air. When inflated, the bladder will cause the actuator to increase in volume but because of the geometry of the mesh as the actuator's diameter increases its length decreases, producing a tensile force.

The BPA's also have several advantages. They typically weigh much less than air cylinders of comparable size. Where air cylinders typically use rigid metal construction, the BPA consists almost entirely of lightweight polymers. They are a contraction-type, single acting actuator similar to muscle. And although the force-to-length curve is not exactly the same as muscle, both these actuators and organic muscles have a force-limiting feature (as they contract fully the

force diminishes to zero). This helps with control and stability of the joint. Also, for a given air supply pressure, BPA will produce greater tensile forces than an air cylinder of a similar diameter. Therefore, the force-to-weight ratio greatly favors the BPA.

In previous investigations BPA's have shown that they have a superior strength to weight ratio compared to air cylinders [11], [20]. This is due partially to the materials used in their construction. Lightweight polymers are the main materials, and very little metal is used. They are very light and flexible. Their high strength to weight ratio and muscle-like properties make them a desirable actuator for biologically-inspired robots. Their maximum strain is similar to muscle, their force output goes to zero as their length goes to the minimum, and they have passive stiffness that can be modulated. However, they do have some shortcomings. Because of the materials used in their construction, they tend to fail in fatigue, often catastrophically [19].

5.2 Bladder

Because of the diminutive size and scale of the robots that were the goal of this project, there was no commercial source of BPA parts and all components were custom made. The latex tubing was made through a process of multiple dips using a stainless steel mandrill and then leaching and baking. The first dip was in a wetting agent that aided the adhesion of the latex to the mandrill. The next step was a number of dips in uncured high quality latex with a very brief curing time between dips. The number of and duration of the dips determined the wall thickness of the finished tubing. The next step was a leaching process that involved a 20-minute soak in 115° F water. Finally the tubing was cured in a 165°F oven for 60 minutes. This produced bladders that were thin, tough and could withstand strains approaching 300%.

Latex was chosen over many other materials because it has a low material stiffness and is capable of undergoing large strains. For the bladder, a lower stiffness is better. If the material is too stiff, too much work is required to stretch the bladder, limiting the contraction of the actuator and its ability to do useful work.

5.3 Mesh

The mesh was woven using a microdeiner polyester yarn made up of a bundle of non-twisted or braided strains of the polyester. The strains are very fine and in the case of these actuators there was approximately 160 strains per yarn in the mesh. In early versions of the actuator, the braiding was done directly over the short pieces of latex tubing. This proved to be wasteful and required many material shipments between suppliers. To eliminate this, parameters were developed so that the mesh could be braided separately and the tubing inserted during assembly at a later time. Philadelphia College of Textiles helped choose the material and develop the proper weave parameters for the braiding. Fiber Architects, a spin-off company from the Philadelphia College of Textiles, supplied the mesh.

5.4 Construction

The basic actuator fabrication procedure was to have the ported end crimped on the fitting and a tendon inserted in the closed end of the actuator. All the fittings for the robot where made from 17-gage thin wall stainless steel tubing. Simply pressing the connecting tubing over the fitting made the connections. The fitting end of the actuator was always used as the origin of the actuator. The origin of the actuator is the end of the actuator most proximal to the chassis of the robot. The insertion is the attachment point of an actuator at its distal point from the chassis. The open end of the actuator did not need a tendon as it was clamped to the structure of the robot. The closed end of the actuator was then inserted on the other side of the joint using the attached tendon. The tendon was wrapped around a constant radius moment arm and fastened under a screw.

Closure of the tubing-mesh combination was done with thin 22-gage annealed steel wire. The wire being annealed was important because we found that stainless steel wire was too brittle after work hardening at the point of twist. The annealed wire did not work harden as much and did not fracture like the stainless steel wire. In the first generation, the actuator's closed end was clamped on a piece of monofilament line with a ball of monofilament melted onto its end to prevent it from pulling free of the actuator. The ball end of the monofilament line was dipped in uncured latex, inserted into the end of the actuator and the mesh and tubing were clamped on the balled end of the tendon with a double wrap and a twist of the steel wire.

The monofilament proved to be too inflexible as a tendon material and hampered joint flexion. After use in the first-generation cricket cart it was abandoned. For the rest of the project, silk suture was used as the tendon material. Actuators with the old and new tendons can be seen in Figure 18. With this change of tendon material the closed end of the actuator needed modification. Simply clamping the silk suture in the end, even with the end knotted, did not work well for either tendon retention or sealing. The solution was to use 1/16-inch OD stainless steel capillary tubing. This has nearly the same OD as the 17-gage hypodermic needle tubing, but with only a 0.015-inch ID. This allows the knotted silk suture to be threaded through the short piece of the tubing. The knotted end is then coated in uncured latex and pulled against the capillary tubing. The tubing is then inserted into the mesh and bladder, leaving the unknotted end of the tendon outside of the actuator and clamped into the closed end of the actuator. This worked well for both sealing and tendon material retention.

The ported end was constructed by clamping the thin wall 17-gage hypodermic tubing used for a fitting with two wraps and a twist of annealed wire. The ported end of an actuator did not require a tendon since it was always used as the origin of the actuator and was clamped directly to the chassis or proximal segment of a joint by means of a collar or split ring clamp. The finished actuator can be seen in Figure 19 and Figure 20.

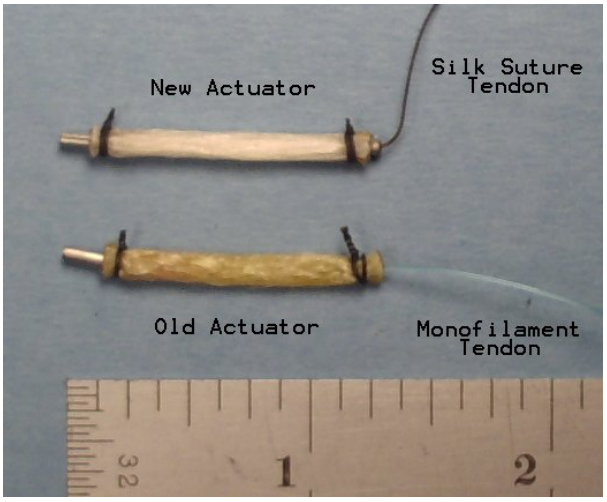

Figure 18. Top: New Actuator. Bottom: Old Actuator.

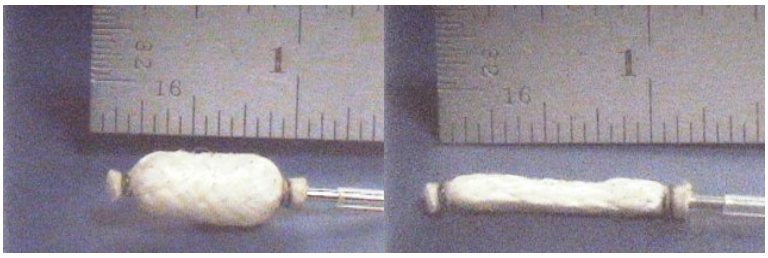

Figure 19. Left: Actuator Inflated. Right: Actuator Deflated

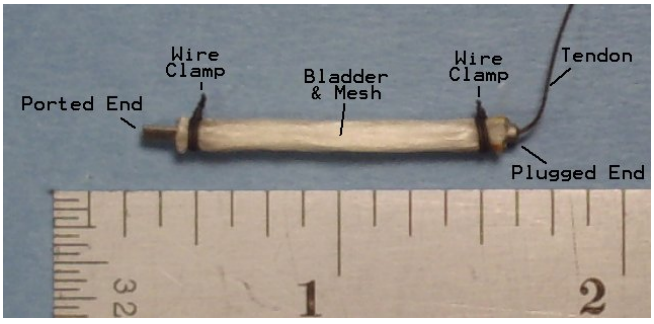

Figure 20. Actuator Parts

One of the problems with this construction was the extremely slippery behavior of the polyester mesh. This would allow an aneurysm of the latex bladder through the mesh that would result in explosive failure of the bladder and destruction of the actuator. This was resolved by putting a thin coating of latex on top of the mesh of the finished actuator. This greatly improved the stability of the mesh and nearly eliminated bladder aneurysms at only a small performance cost as described below.

BPA require an initial activation pressure below which they will not contract. If the internal pressure is below this minimum activation pressure there will be no contraction of the actuator. Once this pressure is exceeded the actuator will function as one expects, contracting with more force as the pressure is increased. This initial activation pressure depends on a combination of initial ID and the relaxed wall thickness. To lower the activation pressure one needs to increase the ID and/or reduce wall thickness. The ID is limited by application size. Using as large an ID as practical is a good rule of thumb. Wall thickness is a compromise between thinner walls to lower activation pressure and thicker walls to increase cycle life. Early actuators had activation pressures around 12-15psi. As the process was refined, activation pressure was reduced to about 7-10psi.

5.5 Results

The final actuators averaged 0.050-inch ID and 1/8-inch OD and they could be made in any length from approximately 0.500 inch to 5 inches, which was the maximum length of latex tubing the dipping and curing process produced. Most actuators used in this project were between 1.00-1.125-inches long, although the six-legged robot uses four 1.375-inch actuators on the front legs.

Figure 21 shows the force-length curve for the actuators built for the robots. The curves are generated using an equation from Chou et al. [8]. Parameters from the actuators were entered in a spreadsheet using Chou's equations to generate the graph. The parameters where then adjusted slightly to fit our empirical data. For comparison, a commercially available 5/32-inch diameter air cylinder at 10psi would generate about 0.19lbs of force and at 30psi about 0.57lbs of force. As seen in Figure 21, the BPAs produce much higher forces, even near the end of their contraction.

By the third year of the project, the actuator design was well established and the actuator manufacturing process had been refined. We developed a process to ensure that the actuators produced were as uniform and reliable as possible. The actuators were characterized by the initial pressure needed to activate them. This number enables actuators to be chosen for mounting depending on the usage requirements. A low activation pressure was always desirable for autonomous operation, but a low activation pressure also indicated an actuator that had a thinner bladder. Higher-activation-number actuators were chosen for use in applications where actuator endurance was more important than performance at low pressure. This was common with the actuators mounted on non-autonomous robots.

The later, thin-walled actuators were far more reliable and had longer cycle lives than those produced earlier. Many of the early actuators would fail after only 50-100 cycles. By the end of the project, we manufactured actuators that lasted several thousand cycles before failure. We also reduced the types of failures that occurred. Early actuators commonly failed catastrophically with bladder ruptures and/or end plug expulsion failures. As the quality of actuators increased throughout the project, we eliminated nearly all end plug failures, and bladder failures were not as drastic. In most cases it was a pinhole failure instead of the larger ruptures in the bladder; so, when the failure occurred, it was not catastrophic. This allowed the

actuator to function with diminished performance. In the lab this is not important because the actuator could quickly be exchanged for an undamaged one, but in the field the fault tolerance of subsystems is the difference between mission failure and success.

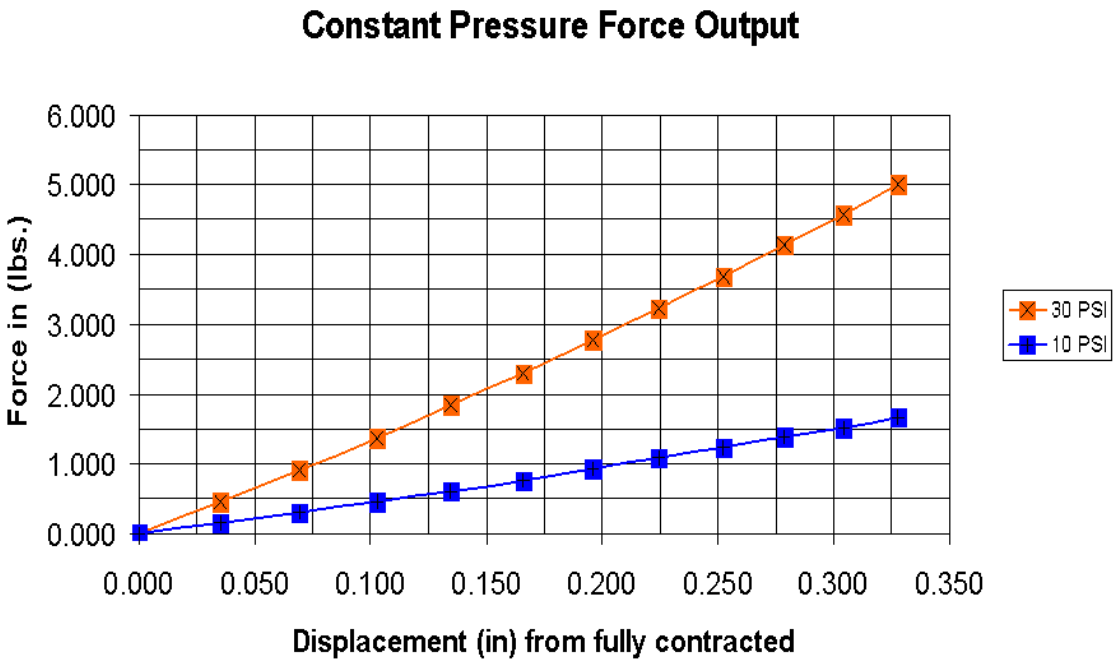

Figure 21. BPA Force vs. Length Curves for Two Pressures.

6. COMPRESSOR

6.1 Introduction

The airflow and pressure needed for the micro-robots was estimated by scaling that needed for Robot III [26], a 30-inch long pneumatic robot in the Biorobotics Lab. The required volume and pressure of air was estimated from the amount required to operate this larger robot using scaling principles. We estimated that about 7psi at 0.1 liters per minute would be needed to operate the cricket robot.

Dynamic scaling based on power requirements for Robot III provided an estimate of the power needed to run the cricket micro robot. The following calculations show the assumptions and parameters used to scale Robot III down to the size of the cricket robot.

When using kinematic scaling to scale up or down the size of a robot, the following assumptions and definitions are used. In kinematic scaling, joints move through the same angles measured in radians, which have no units; the subscript S denotes the smaller vehicle's parameter and the subscript B denotes the bigger vehicle's analogous parameter. Length scales linearly and this ratio of lengths is used throughout this analysis and is defined as

$$l = L_B/L_S \quad (1)$$

Density of the materials is also scaled linearly and the ratio of density is defined as

$$d = d_B/d_S \quad (2)$$

Since mass is a function of both the density and volume of the robot being scaled the ratio of mass is a function of both as

$$m_B/m_S = d * l^3 \quad (3)$$

The assumption that they both are affected by the same gravity leads to time scaling for some equivalent motion as

$$t_B/t_S = l^{1/2} \quad (4)$$

Pressure is a function of force per unit area, with force described in units of mass and acceleration. Since we have assumed acceleration is independent of scale, we have pressure as a function of mass and area. Reducing units results in

$$P_B/P_S = d * l \quad (5)$$

Flow is volume per time and so flow scale

$$Q_B/Q_S = l^{5/2} \quad (6)$$

Power reduces to a function of mass length and time. Reducing units we arrive at

$$\text{Power}_B/\text{Power}_S = d * l^{7/2} \quad (7)$$

$$\text{Power/mass} = l^{1/2} \quad (8)$$

Note that the required power/mass is less for smaller robots. This is encouraging for developing small autonomous robots. The Froude number is used to compare vehicles of different scales. It is defined as follows:

$$\text{Froude number} = v_B^2/gh_B = v_S^2/gh_S \quad (9)$$

We scaled Robot III down to the scale of the proposed cricket robot using the above scaling equations. Robot III is 30 inches long, weighs 30lbs, uses 100psi air at about 3CFM, and consumes power at about 1000watts. The micro-robot was assumed to be 2 inches long, so the length scale factor *l* is 15. The density ratio was assumed to be unity. The resulting 2-inch long robot weighs 0.009lbs (4.1g), requires 7psi air at about 0.0034CFM (0.096LPM), and consumes about 0.076 Watts of power.

It is important to remember that Robot III is not autonomous and cannot jump far. The micro robot will weigh more than 4 grams because it will have all of its systems onboard for autonomy. It will also require more pressure to overcome the initial pressure required to activate the BPA and for jumping. Valve speed limitations will reduce needed flow rate. Because of these factors we specified that the compressor should provide 20psi at 0.1LPM.

6.2 Compressor Design

There are many designs for pneumatic pumps and compressors and each design is optimized for operation at different pressure/flow ratios. The first choice was the basic compressor design. Choices include axial turbines, radial turbines, rotary vain, and reciprocating piston.

Based upon some fundamental calculations it became evident that it would have to be a positive displacement type compressor and a reciprocating piston compressor would be the best choice to achieve the relatively high pressures and low flow rates that were require for this application. A piston compressor is about the only type that would be able to meet the specifications without being overly complicated for the scale required.

The reciprocating piston compressor offers a design that has few high tolerance fits. The only critical fit is the piston-cylinder clearance and as described later in this chapter this problem was overcome by using commercially available parts. The rest of the reciprocation parts are relatively simple to design and machine.

The compressor was originally designed using a 5mm Smoovy brushless DC gear motor. Calculations were done using the gas law to estimate the maximum possible stroke length capable given the available piston diameters and kinematic parameters of the mechanism. Since the design was a simple crank and slider mechanism and the maximum force required to move the piston at maximum output pressure was known, the required torque could be easily calculated.

The calculations were as follows: the manufacturer provided the maximum continuous torque produced by the motor. This was then multiplied by the gear ratio of the attached transmission. The maximum torque produced by the motor through the transmission was checked to make sure it was not larger than the maximum torque rating of the transmission. There is a significant chance for damage to the motor if the maximum torque produced is much greater than the maximum rating of the transmission in the event that the mechanism is seized or stalled for some reason. Once the maximum torque that the motor/transmission could deliver was calculated, the maximum stroke length possible for a given bore diameter could be determined.

The piston diameter was chosen first and then the maximum drivable stroke length was calculated. The choice of bore diameter was limited to commercially available pistons. It was decided that the mechanism and piston should be able to operate with internal pressures of at least 35 PSI. With the extra pressure above the required 20 PSI, it was thought that the robot would be capable of jumping. This also has the advantage of storing more reserve air in a pressure reservoir of the same volume. With the maximum pressure and the piston diameter determined, the maximum force needed on the piston rod could be calculated.

The torque required is a function of the position of the piston, which determines the pressure in the compressor cylinder and the geometry of the crank and slider mechanism. A spreadsheet was constructed that completed a table of pressures and positions for the compressor piston. It was assumed in the worst case that the pressure reservoir was at maximum pressure (35 PSI). Then the simplifying assumption was made that the exhaust valve does not open till the end of the stroke. The initial and final pressures assumed were 0 PSI at the bottom of the stroke and the desired 35 PSI at the top of the stroke. Knowing the initial and final pressures, the percent of the cylinder's initial volume that needs to be compressed to achieve the desired pressure was

determined. This is called the compressor efficiency and it will be revisited when the check valves are discussed. The length of stroke was treated as a variable and a spreadsheet using the gas law was used to calculate the force needed to move the piston from the 0 PSI position to the 35 PSI position.

Now that the force position table was available, it was used to calculate the necessary torques in the crank-slider mechanism. Using the position of the piston and having all the other links of the mechanism determined except the crank length, the torque require was calculated as a function of the crank length. The crank length was chosen at that same time as the stroke length since the stroke length is twice the crank length. Using this geometry, the torque required along the full compression stroke of the piston was calculated (see Figure 22). The 180 degrees in the graph denotes the piston at the bottom of the stroke and 0 degree the piston at the top of a stroke.

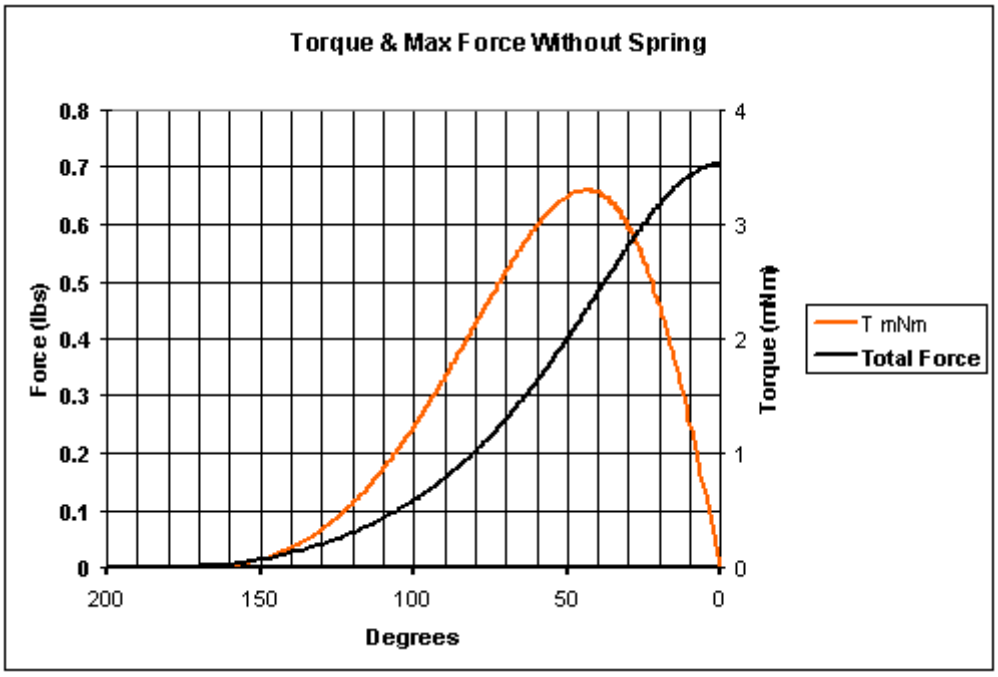

Figure 22. Torque and Force Requirements

Shown in Figure 22, the maximum torque occurs a little over 45° degrees after the crank being perpendicular to the piston rod. Now that the entire spreadsheet was complete, a stroke length can be entered and the maximum required torque could be determined. Thus a manual iterative method can be used to quickly find the maximum length of the stroke possible given a particular motor, transmission, and particular bore size of the piston.

Using this spreadsheet it was determined that for much of a cycle the motor was doing little or no useful work. When it did do useful compressive work, the torque requirement climbed quickly to the limit of the motor. A compression spring was added behind the piston to help with the compression stroke. This helped by allowing the compressor to store energy on the return stoke. The spring was modeled as linear in the spreadsheet. The stiffness and preload for a given spring

was determined experimentally and entered into the spreadsheet as a new section of the table with the spring force being dependent on the position of the piston. Now the force position curve was a combination of the pressure on the front of piston and the spring force on the back of piston (see Figure 23).

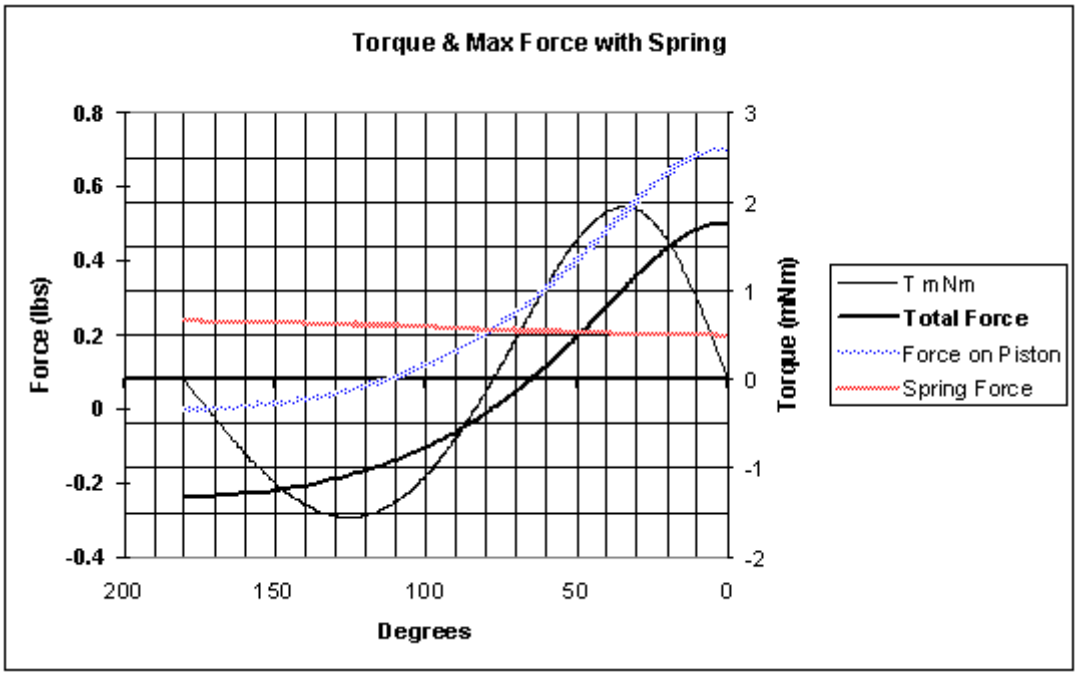

Figure 23. Torque and Force for Compressor with Spring

The spreadsheet provided a good approximation, but several important factors that were not easy to calculate were ignored. First, this assumed adiabatic compression, which probably was not true, given the high cycle rate of the compressor. Also, viscous losses of the check valve assembly were not taken into account. Other losses not directly calculated were friction along the cylinder walls, piston rod, and at the mechanism's joints. In the first generation of the compressor, transmission efficiency was also overlooked but this was approximated in a later version of the spreadsheet. This approximation also fell short in later generations of the compressor, which used transmissions with plastic gears. At high loadings, these transmissions caused the efficiency number to drop significantly below the efficiency numbers specified by the manufacturer.

Despite all these shortcomings, the spreadsheet was a useful tool in the design of the compressor. The inaccuracies forced the use of a shorter crank than the spreadsheet indicated the compressor could operate with. Even with the shorter crank, if the compressor efficiency was at or above the required efficiency, it still operated as calculated, except with a lower flow rate. Flow was a shortcoming of the compressor, but maximum pressure was not. This was due to the way the design space was explored and the fact that the stroke length was the last parameter determined. We made pressure the dominating specification and flow was sacrificed to obtain the pressure. If we had wanted - the stroke could have been kept as calculated and the losses not accounted for in the spreadsheet would have resulted in a lower than anticipated pressure.

6.3 Fabrication

Fabricating the piston and cylinder would have required significant amounts of machining time because of the close tolerances required. Commercially available air cylinders were modified and used for the compressor piston and cylinder walls. In the first two versions of the compressor, 5/32 bore air cylinders from Clippard were used (see Figure 24). In the last version a Clippard ¼ inch bore air cylinder was used (see Figure 25).

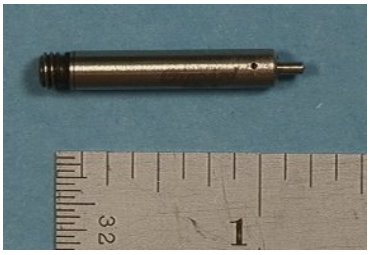

Figure 24. Clippard 5/32 Bore Air Cylinder

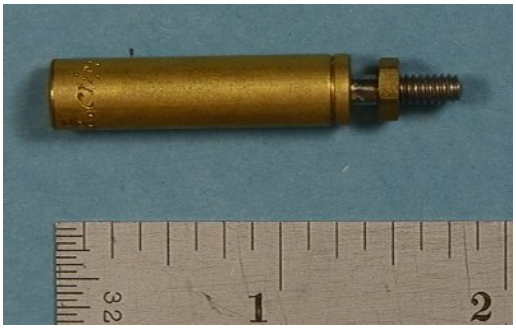

Figure 25. Clippard 1/4 Bore Air Cylinder

The maximum stroke available for the Clippard 5/32 bore air cylinder was 0.5 inches. The 5mm Smoovy gear motor (see Figure 26 Left) came in one of three available transmissions with gear ratios 25:1, 125:1, and 625:1. The 25:1 was chosen for several reasons. If a high transmission ratio was chosen, the motor could actually damage itself if the mechanism stalled. Also, the more stages the poorer the efficiency of the transmission. The drawback to the low transmission ratio is that at high output RPM frictional loses are higher due to higher velocities of the piston. The check valves must also be able to react quickly enough to keep up with the fast changing flow or more energy losses would result.

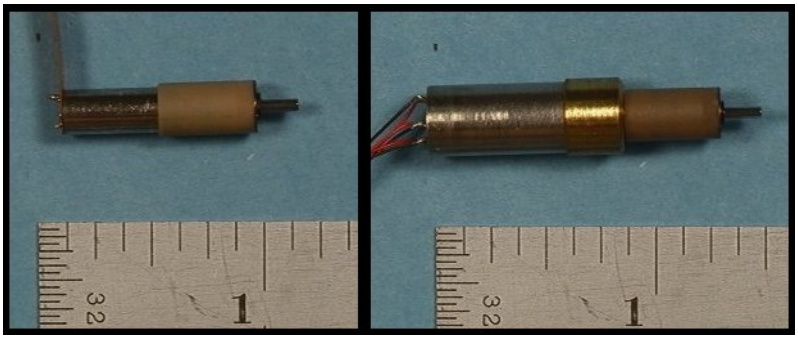

Figure 26. Left: 5mm Smoovy. Right 8mm Smoovy. Both With 25:1 Transmission

The overall design was a simple crank and rocker mechanism (see Figure 27). The crank in the first version was machined from aluminum. The aluminum crank had a press fit axle and one hole tapped for a 0-80 cap screw that engaged the flat on the transmission shaft. This was later changed to brass because a denser material was needed to help incorporate a counterweight into the crank. Later versions had one screw to engage the flat on the gear motor output shaft and another tapped hole to support a screw through the axle shaft.

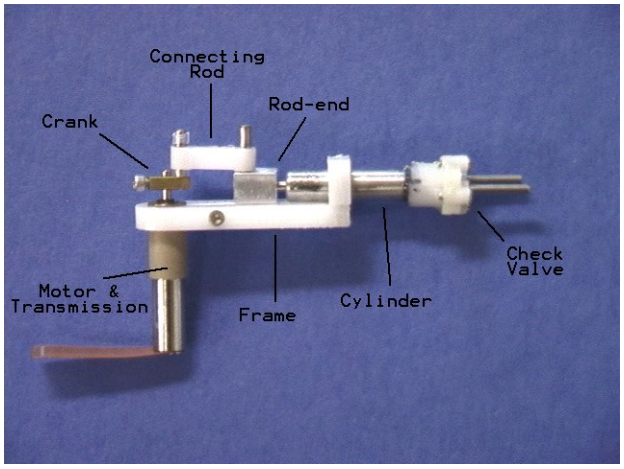

Figure 27. Compressor Components

The connecting rod was machined from Delrin with a bushing at each end that would slip over the crank axle and rod-end axle. Hypodermic needle tubing was used for axles. The Delrin in the connecting rod acted as a bushing material.

The rod end for the 5/32 bore piston was made from aluminum and in the first generation had a press fit axle and a screw to clamp the rod end on the end of the piston rod. The rod end was later upgraded to a screw-supported axle. These two types can be seen in Figure 28. The ¼ inch piston was used in the last version of the compressor, since the end of the piston rod was threaded. The rod-end was changed to a yoke design, machined from Delrin and threaded onto the end of the piston rod.

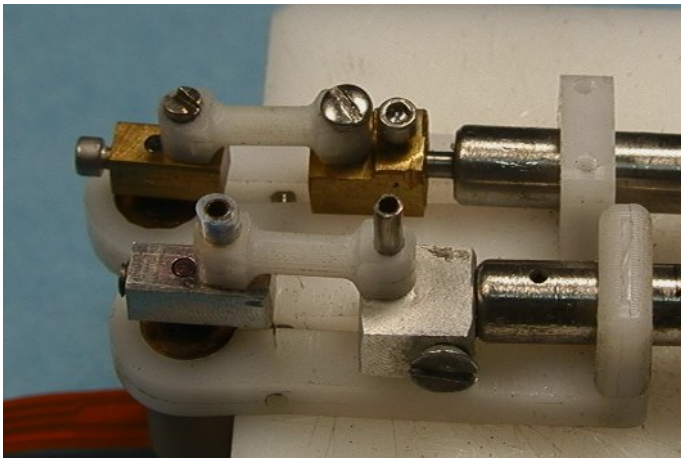

Figure 28. Bottom: Press Fit Axles. Top: Screw Supported Axles

The first generation compressor's cylinder was made of stainless steel with 1/64-inch thick walls and a 5/32-inch ID. The piston rod was a 1/16-inch stainless steel shaft and piston that used a "C" cup O-ring for a seal against the cylinder wall. Later versions of the compressor used a ¼-inch bore piston and the cylinder walls were 1/32-inch thick brass with a stainless steel piston and piston rod. It also used a "C" cup O-ring.

The first successful compressor used a very short crank arm having an effective length of only 0.08 inches (see Figure 29). This resulted in a 0.16-inch stroke which was less than calculated, because of the frictional losses at joints and piston walls and transmission efficiency was not taken into account. The axles on the crank and rod ends were pressed into place and were cantilevered. The line of force from the crank through the connection rod was out of line with the center of the piston, producing unnecessary moments. It developed over 40 PSI, but flow rates were well below what were needed.

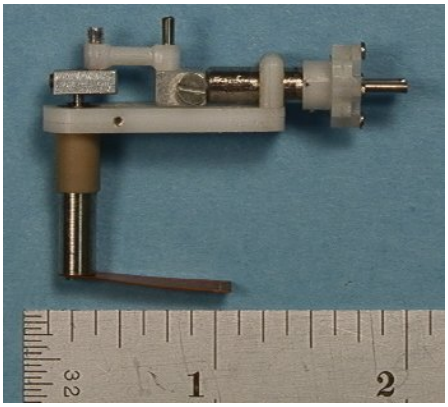

Figure 29. First Successful Compressor

6.4 Check Valves

The check valves were the most challenging part of designing and building the compressor. The design progressed through 7 different iterations before a design was found that could perform in the desired pressure and frequency ranges (see Figure 30).

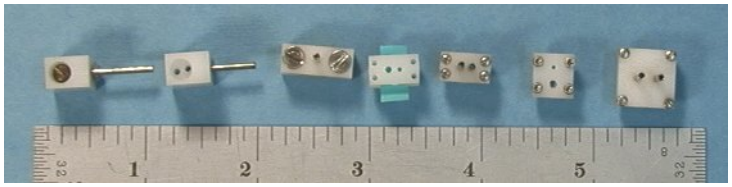

Figure 30. Many of the Failed Check Valve Designs

Many commercially available compressors use actuated valves. This has several advantages including increased efficiency and flow, slightly higher pressures, and compared to a similar passive valve the actuated valve has a lower head loss. The disadvantage is the complexity of the mechanism that actuates the valves. At the scale of most commercially available compressors the complexity of the actuated valves is easily offset by the boost in performance. At the scale of the compressor needed for this project the frictional losses due to this extra level of complexity is greater than the benefits achieved.

The final design was a simple trapped flapper valve design that put two flapper valves in opposite directions, one the inlet and one the outlet. The final design of the check valves can be seen in Figure 31. Each flap was trapped in a cavity that had a hole above and below the flap. The one side of the cavity had a smooth surface around the hole. The other surface had a groove through the hole that extended beyond the edge of the flap. When the flow moved in the direction of the smooth hole the flap would seal the hole and hold pressure. When the flow reversed the air would pass around the flap by means of the slot that connected with the hole in that face. The final design was simple in concept but the implementation was a challenge at this scale. To get the desired pressure, approximately 72% compressor efficiency was needed. This is not high volume efficiency, but when the piston is 5/32 inch in diameter, it is a challenge to get the valves close enough because a high efficiency requires that the valves be very close to the top dead center of the piston's stroke. The final valve package put the valves within approximately 1/64 of an inch of the top dead center position of the piston. Another constraint was that the two ports for the check valves had to fit within the confines of the 5/32 inch bore. Because of these constraints, the flaps were 0.100 inches square and made from 0.007 inch thick latex cut from latex gloves.

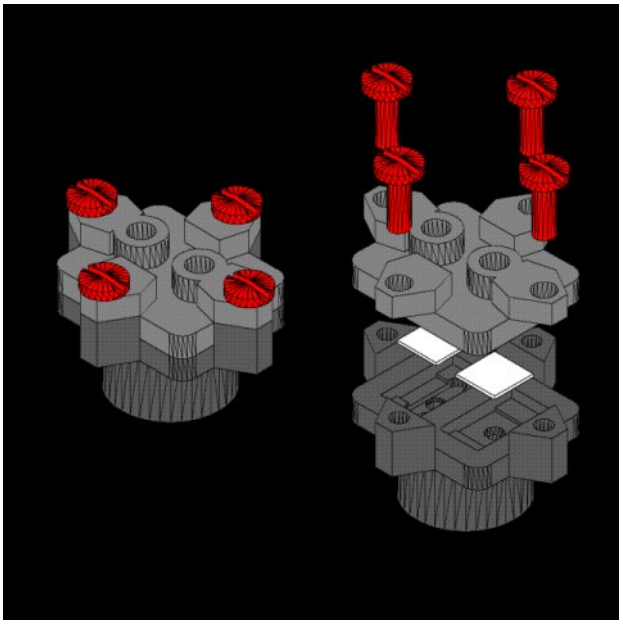

Figure 31. Dark Gray: Base. Light Gray: Lid. White: Flappers. Red: Screws

Sealing the package proved to be the greatest challenge. The package was machined from two pieces of Delrin. The base part was pressed onto the cylinder walls and sealed with superglue. The flappers seated and the mating faces of the two halves of the package had 1/64 inch wide grooves milled into them to help seal them together. These grooves were then filled with uncured latex and allowed to dry. A second coat of latex was put on one side and the valves were assembled with four 00-90 screws and allowed to dry. The latex acted as a gasket and created a good seal.

6.5 Results for the Smoovy Motor Compressors

Without any way to store energy, the required torque to operate the compressor was too large. To solve this problem a spring was added to help during the compression part of the cycle (see Figure 32). Energy stored in the spring on the return stoke is used to help compress the air. This reduced the maximum torque required.

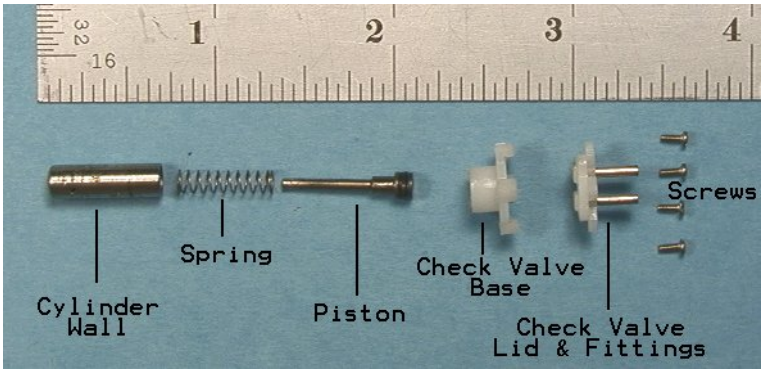

Figure 32. Components of Cylinder

The next generation of the compressor used all the same components except the motor. The first generation used a 5mm Smoovy motor, while the second generation used a 8mm Smoovy motor. The 8mm motor was not used previously because at the time of design there were no transmissions available for it. Smoovy supplied a prototype coupler that allowed their 8mm brushless DC stepper motor to connect to their 5mm gear head. This helped to increase the available torque by a factor of 6. The extra torque supplied by the 8mm motor allowed the full 0.5 inch stroke to be used and greatly increased the flow rate of the compressor. The flow was still less then the desired amount, but it was much greater than that of the 5mm motor version. See Figure 33 for a comparison of these compressor's flows at different pressures.

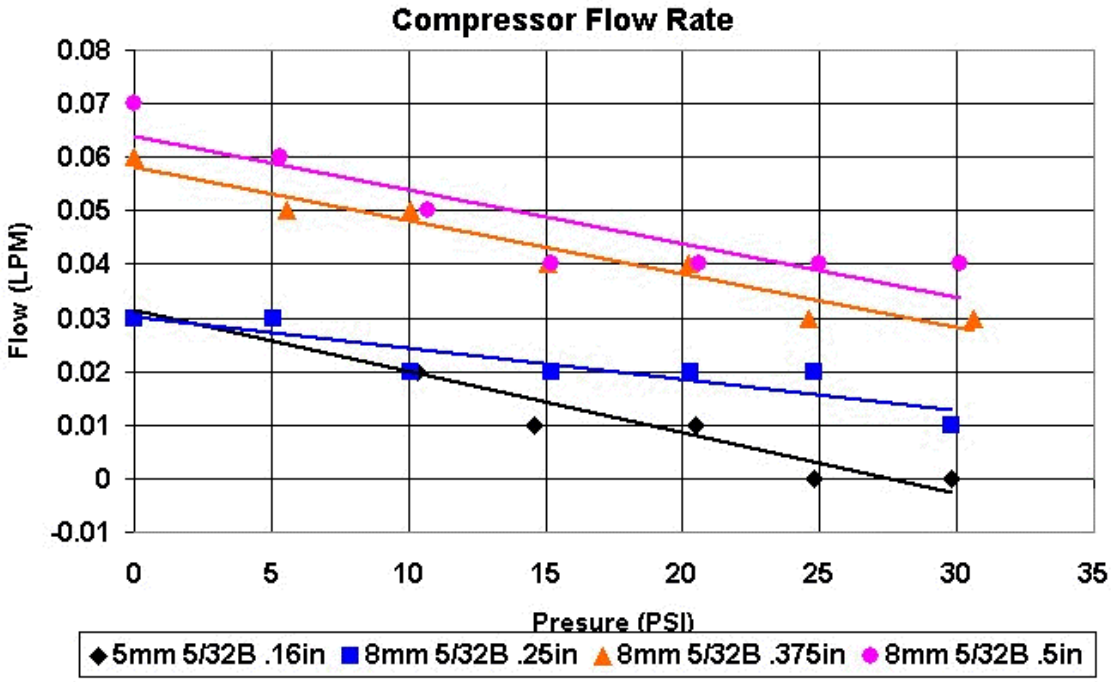

Figure 33. Flow vs Pressure for 5mm & 8mm Smoovy Compressors

The biggest shortcoming of using a Smoovy motor had nothing to do with the motor, but the controller that they supply for it. Smoovy makes a very small controller constructed of surface mount components and is only about 0.75 inches square. The problem with this controller is that it does not have feedback and it merely sends feed-forward commands to the motor. The problem is without feedback there is no way of telling if it had stalled. Once the motor did stall, with the high torque requirements of the application, the motor would never recover and the controller and compressor would need to be restarted. Smoovy did have a feedback controller that greatly increased the torque by pulling and pushing with two of the three poles of the motor. The controller then used the third pole for position feedback by sensing the back EMF from the inactivated coil. This controller however, did not use surface mount components and was 4x3.125 inches and weighed nearly as much as the finished robot. This controller weighed 66 grams. As part of the project, the proprietary controller chip was removed from the Smoovy board and remounted on a smaller board with the equivalent surface mounted components. A size comparison can be seen in Figure 34. We were able to reduce the weight by 58.5 grams to 7.5 grams on a circuit board that is 2 x 1 inches.

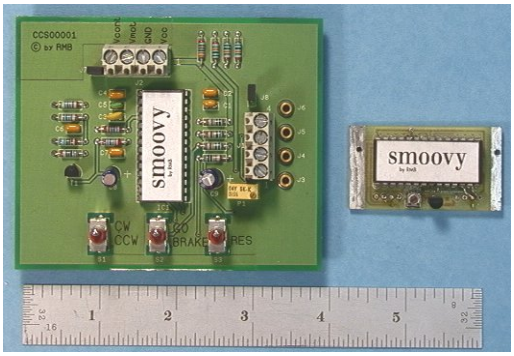

Figure 34. Left: Original Controller. Right: Remounted Controller Chip

6.6 Final Compressor Design

As construction started on the second-generation cricket cart robot, we redesigned the compressor again. Maxon had released a new 10mm gear motor that was not available when the original design of the compressor was made. The weight of the 10mm motor was heavier than the 8mm Smoovy but because it was a brushed DC motor it did not require a stepper controller and the resulting system weight was less. The 10mm Maxon motor weighed 12.5 grams. The Smoovy motor weighed 7.6 grams with an additional 7.5 grams controller for a total of 15.1 grams. The new Maxon motor could deliver more torque and thus a more powerful version of the compressor could be produced (see Figure 35). The Maxon motor produces 1.54 mNm of torque. The 8mm Smoovy motor produces 0.65 mNm of torque and the 5mm Smoovy motor produces 0.11 mNm of torque. At the transmission output the Maxon motor output is 24.6 mNm (16:1), the Smoovy 8mm motor output is 16.5 mNm (25:1), and the Smoovy 5mm motor output is 2.75 mNm (25:1). The piston was increased from 5/32 inch to ¼ inch with a .219 inch stroke.

Again the compressor didn't perform quite as well as hoped, with the shortcomings coming from degrading transmission efficiency due to high torque and plastic gears used in the transmission. The gears used in Smoovy transmissions are brass, but the ones in the Maxon transmissions are nylon. The efficiencies quoted in their specifications are only accurate up to a certain torque and then the efficiency drops sharply due to gear deformation. Nonetheless, the original goal for the compressor of being able to deliver 0.1 LPM at 20 PSI was now met (see graph in Figure 36). The maximum pressure limit of the compressor also increased to nearly 50 PSI.

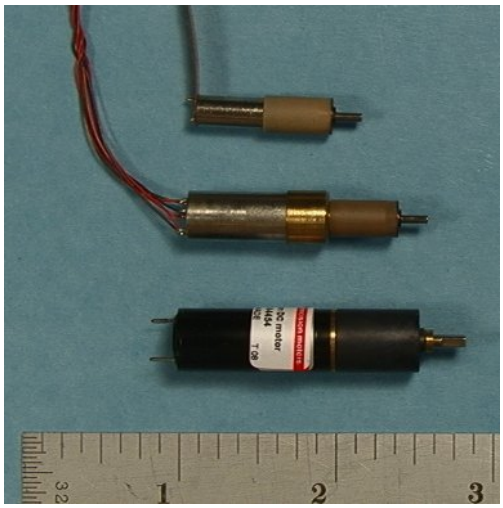

Figure 35. Top: 5mm Smoovy Motor. Middle: 8mm Smoovy Motor. Bottom: 10mm Maxon

The larger diameter piston and cylinder made construction and machining of the check valves much easier. The valve package was increased in overall size, allowing six screws for assembly (see Figure 37). The flapper size was increased to 0.125 inches square and the material was switched from Latex to Nitrile. The Nitrile was the same 0.007 inch thickness as the latex, but the material has a higher modulus making it stiffer and less likely to be sucked through the larger orifices in the new valve package. This better material for the flapper and the larger diameter were the primary reasons for the 25% increase in maximum pressure achievable and higher flow rates. The larger size also made making the gasket seal easier by increasing the contact area of the two halves of the package and increased the width of the sealing grooves to 1/32 inch.

The compressor using the Maxon motor used larger diameter axles. The first Smoovy motor compressor used 17-gage hypodermic needle tubing where the later Smoovy compressor and the Maxon motor compressor used 15 gage tubing for axle material. This reduced bearing pressure and lessened the frictional losses at the joints. It also allowed the choice of an axle diameter that let the axle be fastened by passing a 0-80 screw though them rather then press fitting them onto the crank and rod end. The rod end was changed to a yoke configuration to put the force of the linkage more inline with the center of the piston (see Figure 38). This reduced binding in both joints and piston rod.

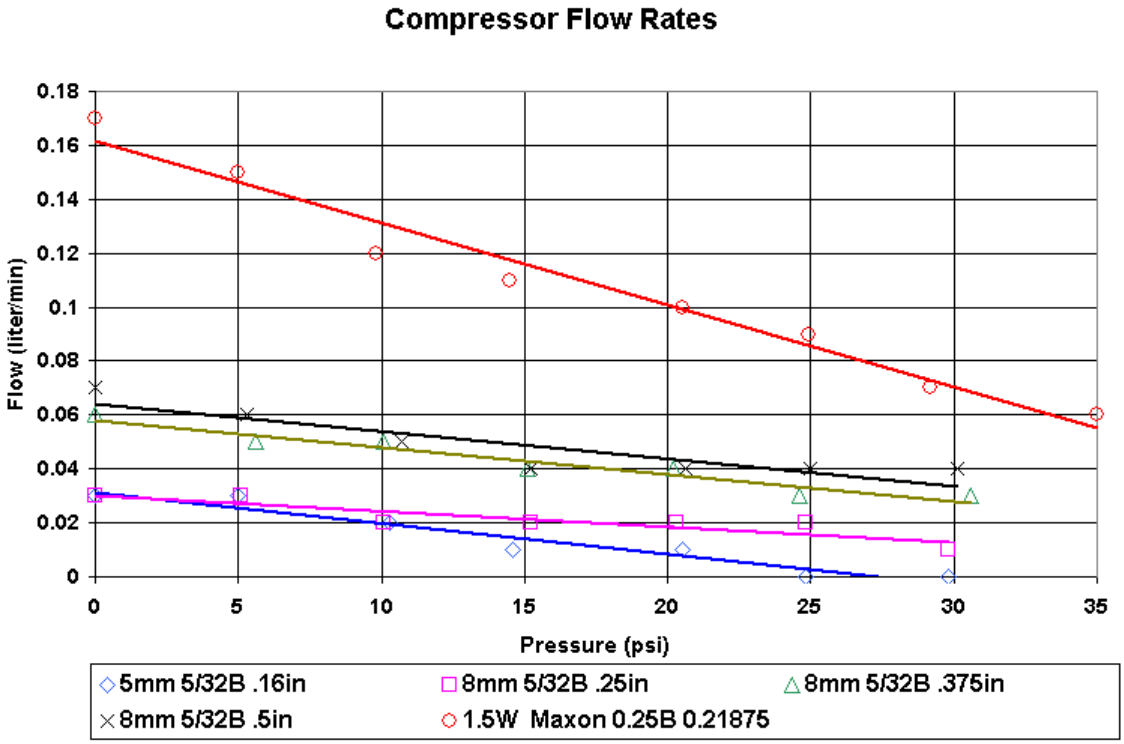

Figure 36. Flow Comparisons for All Three Compressors

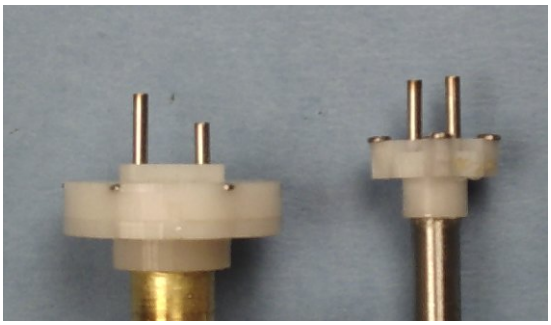

Figure 37. Left: Maxon 1/4 Piston Check Valve. Right: Smoovy 5/32 Piston Check Valve

The new compressor was significantly larger than the first, being almost twice as long as seen in Figure 39. But the overall weight was not greatly increased when the controller required for the Smoovy motor is taken into account. It is difficult to determine exact weight differences because the frame of the compressor was integrated into the chassis of the robot. However, we can compare the standalone versions. The 5mm Smoovy compressor weighs 9.2 grams (16.7 grams with controller). The 8mm Smoovy compressor weighs 18.5 grams (26 grams with controller) and the Maxon Compressor weighs 39.5 grams (requires no controller).

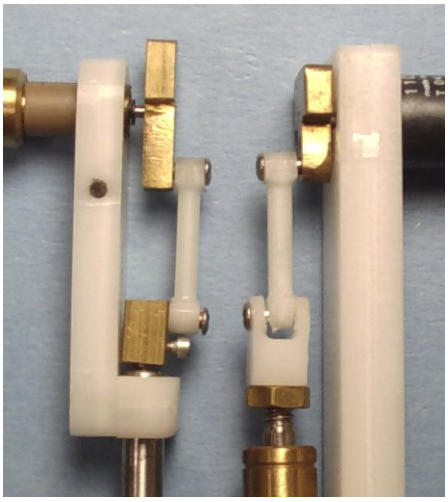

Figure 38. Left: Original Design. Right: Yoke Design

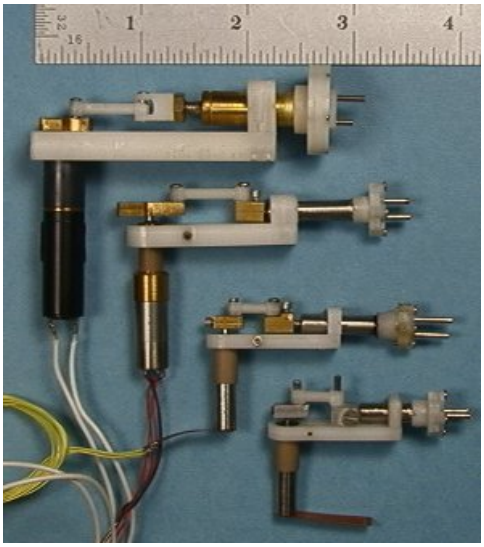

Figure 39. Bottom to Top: First Operational 5mm Compressor, Improved 5mm Compressor, 8mm Compressor, Maxon Compressor

7. MICRO VALVES

Valves are necessary to port air to the actuators from a tank of compressed air. We designed a three-layer, two-way valve that was made using a MEMS batch fabrication process [5]. Two of these devices need to be packaged together to form one useful four-way valve for each actuator. The design consisted of a passively closed orifice valve that used a TiNi actuator to open the orifice [5].

The three layers of the valve were built up as follows (see Figure 40): The first layer (the bottom layer) was the orifice plate. A small 500 micron hole was etched though the plate. The next layer was the actuator layer. A plunger that closes the hole in the orifice layer is suspended in a

ring of silica and on a filament of TiNi wire. The third layer (top layer) was a double spiral silica spring that pushed down on the plunger passively sealing the valve. To open the valve you apply a current to the TiNi, heating it and pulling the plunger up, opening the valve. All three components are batch micro-fabricated using silicon substrates.

A TiNi SMA actuator was chosen because its high strains (3%) and actuation forces (work density of 5×10^6 J/m^3) enable high fluid flow rates and high working pressures, respectively. The transformation temperatures and strains are very sensitive to compositional variation. Since the Ti and Ni constituents in alloy sputtering targets have different sputtering yields during deposition, a co-sputtering procedure has been developed which uses an alloy TiNi target and an elemental Ti target to reliably achieve stoichiometric SMA films [10].

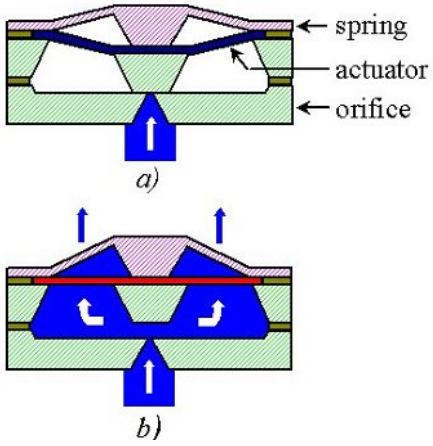

Figure 40. Top: Valve Closed. Bottom: Valve Open

The valve is normally closed. The patterned TiNi actuator and silicon spring allow "flow-through" operation. The spring provides an initial closing force against the orifice making the valve normally closed when the SMA actuator is in its low temperature martensite phase (Figure 40a). When the actuator is heated, it transforms to austenite, forcing the spring upward, opening the valve (Figure 40b). The orifice die simply contains a square inlet.

The microvalve components are fabricated using bulk micromachining, co-sputtered thin film deposition, and deep reactive ion-etch processes. A plasma dry etch and a XeF_2 etch are both used to release the TiNi SMA thin films.

Flow rates of up to 0.5 lpm are achieved for an input air pressure of 245 kPa and the leakage is less than 0.005 lpm, which is the resolution of the flow meter. The microvalve is actuated with 100 mA and the power consumption is 370 mW. The time response of the microvalve controlled pneumatic actuators is acquired using digital video recording, due to the flowmeter's time response limitations. The on time is about 100 msec and the off time is about 150 msec. The fatigue of TiNi SMA actuator is less than 5% after over 1 million cycles of actuation.

In the first generation microvalve design the three primary layers were wafer-scale microfabricated (Figure 41). However, the spacers required resulted in a die-level (single valve) manual assembly operation. In order to take advantage of batch microfabrication, a wafer-scale

assembly approach was pursued. As part of this approach the integration of the spacers with the three primary layers was required as shown on the right side of Figure 41. The most challenging layer is the spring layer. Our approach for this layer was to first perform a wafer-scale bonding of the spacer thickness to the spring wafer. This has been completed successfully. Following this, we perform the deep reactive ion etch step for the spring as in the original design. For the next level we have improved on our original processing by incorporating XeF2 dry etch for the actuator. This process is more reliable than the original processing and has been completed successfully. For the orifice layer, we augment our original wet processing for the orifice with an additional wet etch from the opposite side to form the required spacer. This relatively standard double sided wet-etching technology has been successfully completed. Finally, the three layers with integrated spacers are wafer-scale bonded to complete the valves. The current generation of wafer bonding equipment is reported to handle this level of integration without major obstacles. Our only constraint here is to avoid high temperatures (above 400C), which could damage the TiNi shape memory alloy actuator. Note that the wafers can then be diced into individual valves or into groups of valves on a single substrate for later packaging.

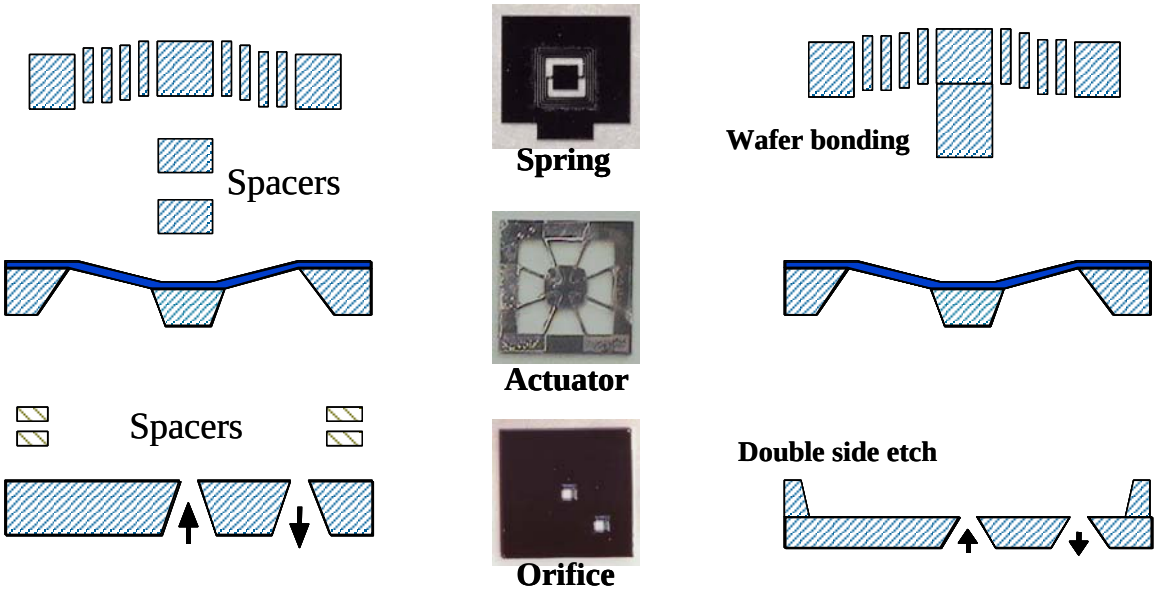

Figure 41. Left: First Generation Microvalve Design Uses Many Spacers. Right: Second Generation Valve Has the Spacers Incorporated Into the Three Major Components.

For MEMS fluidic devices, packaging is one of the key elements that determine the final performance of a device. Our first prototype packages were machined from Delrin or Plexiglas and only held one MEMS device (see Figure 42). The Plexiglas was more difficult to machine, due to Plexiglas being very sensitive to milling feed and spindle speeds; but if done correctly, limited visual inspection of the final assembly could be achieved through the package. The early packages involved sealing the bottom orifice layer of the valve assembly to the bottom of the package and giving porting to both sides of the valve for inlet and outlet flow. To seal the bottom plate around the lower orifice, a 3/32 inch OD 1/32 inch thick o-ring was used. The top

piece of the package was then sealed with a special tape making the package airtight except for the port on the topside.

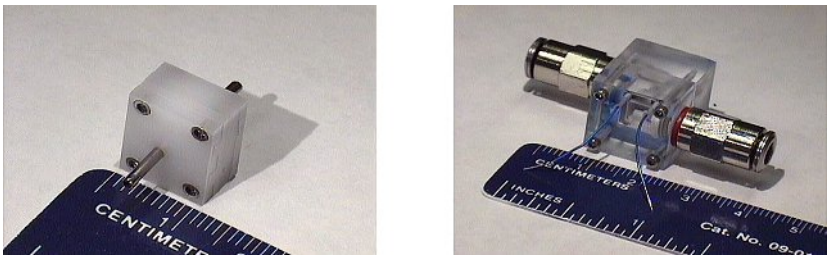

Figure 42. Early Test Packages

For the actual valve package to make the four-way (used as three-way) valve for the robot, Delrin was used to machine a three-layered package that sandwiched two MEMS valve devices in such a way that the valve function as desired. The desired functions are the ability to shut off supply with the actuator vented to atmosphere, shut off the air supply while holding the pressure in the actuator, and finally the ability to connect supply pressure to the actuator (see Figure 43).

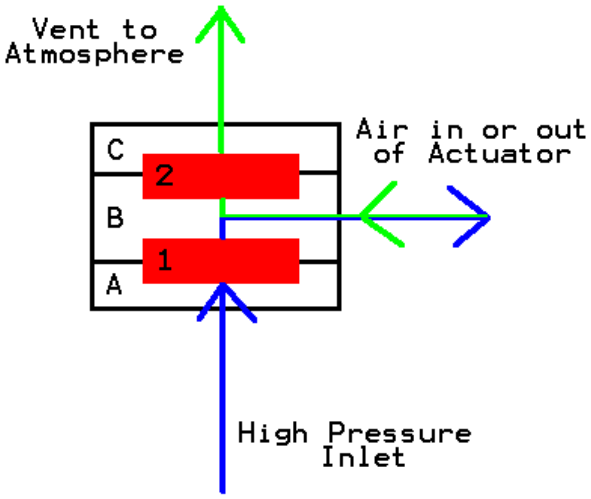

Figure 43. MEMS Device Package Arrangement

In an attempt to reduce the number of fasteners and make the actuator port easy to place, a three screw per layer arrangement was used on the first version of the package (see Figure 44). This provided sufficient force to close the package but the non-symmetrical pressure deformed the lids making them leak. To solve the leakage problem a four-screw package was designed.

Figure 44. Three Screw Valve Package

Finally, realizing that the fewer fittings, the lower head loss and the fewer places to leak, four bases were machined into a lid for the second generation cricket cart's pressure manifold (see Figure 45). This eliminated four sections of hose and eight connections at the cost of a complex piece, but did simplify the system.

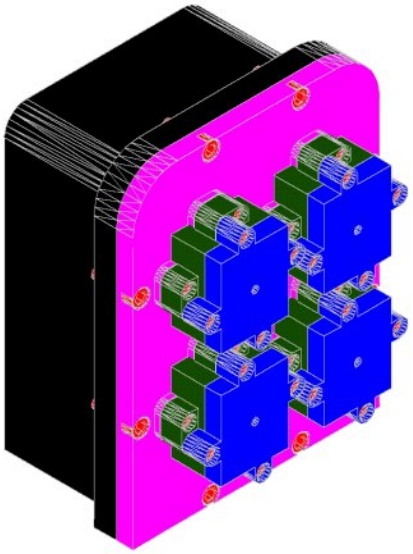

Figure 45. Tank and Valve Assembly Drawing

8. PROTOTYPE LEG

We knew that we would have to keep the robot as simple as possible to be able to achieve autonomy, so early in the planning we decided to keep the legs as simple as possible while still achieving the level of mobility desired. Based upon cricket mechanics and behavioral studies performed in the Ritzmann Lab, the six-legged robot would have simple, powerful back legs and slightly more complex smaller front and middle legs. The rear legs would provide the majority of the thrust to propel the robot and the front and middle legs would support the weight and maneuver the body. The rear legs were designed with two degrees of freedom because it was found that a cricket's rear leg could perform its functions with two segments and two degrees of freedom[22]. This is the simplest leg that permits stance, swing and the transition between. A fixed function leg could be produced by coupling these two joints (with a four bar mechanism for example), but this was not done because some limited flexibility in the length of stance and swing was still desired, and two independent degrees of freedom would allow just enough flexibility to control the length of phases while still being as simple as possible.

Early in the project, as the actuators and other technologies were being developed, we built the first prototype cricket leg (see Figure 46). After doing a kinematic study of the cricket's locomotion, we found that we could reduce the degrees of freedom of its legs in order to reduce its complexity. The rear legs would have two DOF and the front and middle legs would have three degree of freedom each. A prototype rear leg was built to test the actuators and their control. It mounted to a simple base and used braided pneumatic actuators (BPA) for extension of joints and antagonist linear (extension) springs for flexion. A series of tests were done to show that the leg was controllable and powerful. The tests included a repeatability test and a kick test. The prototype performed very well in each of these tests.

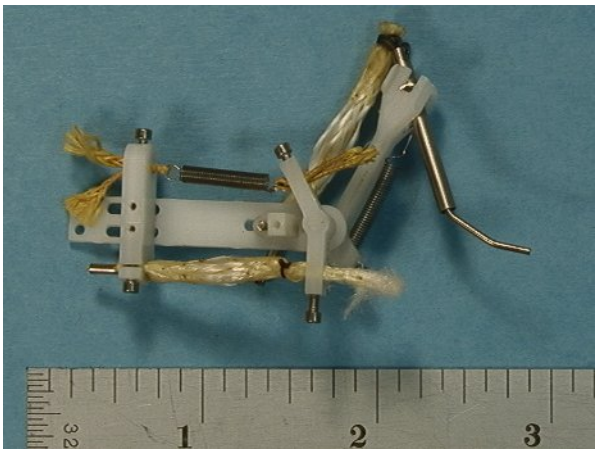

Figure 46. Picture of Prototype Leg

In this prototype leg, a crude femur was made from Delrin. The tibia was constructed by hand from stainless steel wire and tubing. The tarsus was simply a piece of music wire. The actuators were rigidly mounted using a clamp on the originating end and a stiff wire hook on the insertion end. As mentioned above, the antagonist was an extension spring. The insertions were attached to straight moment arms, which resulted in a change of moment arm length during actuation.

Later versions of the legs would use tendons wrapped around constant radius moment arms. The effect of a changing moment arm is reduced range of motion and weaker performance in comparison to later versions of the leg, but this early setup demonstrated that the actuators could be built, mounted and used at this small scale.

Three tests were performed to test the usability of the leg design and actuators. The first was a simple joint excursion test in which we ran the leg through a walking motion and compared the joint angles to those measured on the insect. The leg repeatedly stayed within ten percent of the insect's joint flexion, extension, and excursion. The leg was cycled over a hundred times during which it met this criterion. The next test was a foot-fall pattern test. The leg was mounted in an orientation similar to that of the cricket and a camera was placed so it could look from the bottom up at the leg. The leg was then cycled like it was walking and the path the leg traced was measured against a scaled path from the animal. The leg was also able to do this within ten percent. These first two tests demonstrated that the two DOF rear leg design is sufficient for walking.

The actuators and leg were also tested for strength and the ability to move quickly, as would be required for jumping. In this test, the leg was positioned to use the femur-tibia joint to kick a large paperclip up into the air. Since the valves were not capable of opening quickly enough for the kick, a retarding mechanism was used. The retarding mechanism would hold the tibia stationary until the actuator was nearly at maximum pressure. This test put the leg in a position to kick a large paper clip having a mass of 1.2 grams straight up. The height was measured using a high-speed camera. The leg, in a trial of 20 kicks, averaged a height of 4.61 inches with a max of 5.25 inches. Although the leg's kinematics are sufficient for kicking, this kicking power must be increased to propel the robot a significant distance.

The leg showed both promise and room for improvement. The actuators, although still fragile and temperamental, were strong. The legs, although crude and bulky in construction, operated smoothly and within the desired ranges of motion. The prototype leg showed that controlled powerful motion was achievable. It also indicated things that needed to be refined. The actuator needed longer endurance. Both spring and actuator attachment needed much improvement. It was a healthy steppingstone in the project which also indicated directions for future work.

9. PROTOTYPE CART

9.1 Introduction

After developing much of the aforementioned subsystems, it became evident early in the project that most of these subsystems would not immediately be capable of supporting the complexity and power requirements of a six-legged autonomous robot. So in the first year of the project it was decided to make a compromise and first produce a hybrid wheel-leg vehicle. This compromise would serve several functions. First and foremost, it would be a stepping-stone toward the ultimate goal of producing an autonomous six-legged micro robot. It would further allow us to integrate all the subsystems and solve integration problems, while also giving us time to improve the performance of the sub systems. The hybrid robot would have all the same

systems but the demand on each system would be less than the six-legged robot would require. This would allow a less demanding test of the integration of the subsystems.

It was also hoped that the hybrid robot might be an end in itself. If the vehicle proved to be robust and capable enough on its own it was hoped that the hybrid robot might be a vehicle with some of the advantages of both wheeled and legged robots. The following sections represent work that was done based upon this compromise.

A prototype cart was the first simple proof of concept vehicle created as part of the project. The cart tested the concept of a wheeled cart propelled by a pair of legs mounted on the aft end of the chassis. It has an umbilical that supplies air to the vehicle that used wheels to support the front of the chassis, while it was propelled by a pair of legs mounted at the aft. The legs were modeled after a simplified cricket's rear legs.

The prototype cart was another intermediate steppingstone, as we ramped up to create the first autonomous vehicle. The prototype cart was built as the power-plant subsystems were being developed. The prototype cart would let us show that two-legged locomotion would be possible while at the same time exploring some mechanical aspects of the cricket. As described later in this section we did a detailed study of the rear legs of the cricket while it walked. This study was then applied to a unique pair of two degree freedom legs used in the construction of the prototype cart.

Study of the cricket was done with high-speed videography [22]. We analyzed these data and were able to show that during walking, the cricket’s rear legs moved using two major degrees of freedom. Further analysis showed that the leg motion was nearly planar, except for short periods at the beginning and the end of stance, during which it was slightly out of plane. Because of these results, we decided to use two degrees of freedom and see if capable locomotion resulted.

9.2 Cricket Leg DOF

We collected three dimensional data points from a walking cricket. The data collected were from points marked on the crickets legs and body. The points marked were located at all the leg segment joints and several on the body for reference and orientation. We then digitized the data to determine x,y,z locations of each of the points during the motion. The data were then filtered the data to smooth the noise from the digitization process [22]. The data were than transformed from the inertial reference frame, where the points were collected, to a moving body reference frame. In the coordinate system on the body X was forward, the direction of travel. Z was up, dorsal from the animal. Y was then out the left side of the animal.

We produced an array of vectors that denoted the various points of interest on the animal. Having watched the video of the cricket walking it was observed that the leg appeared to behave much like a two degree of freedom leg and even possibly a two degree of freedom planar leg. With this assumption we hoped to show that the leg did behave like a two degree of freedom leg for much, if not all, of its walking cycle.

The actual cricket leg has four major sections. The most proximal to the body is a very short segment called the coxa. The next segment is the femur, a long heavy section of the leg. Next is the tibia, similar in length to the femur but much more slender. And finally is a very compliant

multi segmented part called the tarsus or foot. Since the coxa was so short the segment was ignored in this analysis and its degrees of freedom were incorporated into a joint called the body-femur joint that incorporates all the degree of freedom between the body-coxa and coxa-femur joints. The tarsus was also ignored since its function is not to propel the animal but to provide a compliant interface with the substrate the animal is walking on. Although it performs an important function during locomotion it does not directly affect the kinematic arrangement of the other segments. With these assumptions, we have a simplified model of the rear leg that has only two segments. The femur attached proximally to the body and at its distal end the tibia. The natural position of these leg segments in the animal is that the femur rises from the body femur joint pointing up and aft on the animal slightly splayed out from the medial plain of the animal. The femur-tibia joint is at the end of this segment and the tibia continues to point aft but is now point back down toward the ground where the tarsus would contact the ground.

The femur-tibia joint is a single degree of freedom hinge joint. What we wanted to show with the following analysis is that during the walking cycle the body femur joint rotates around a single axis of rotation thus giving us a two degree of freedom leg. To do this we used the vector data from high-speed video of cricket walking. These data contained two vectors in the body reference frame. The first pointed from the body-femur joint to the femur-tibia joint, and the second from the tibia femur joint to the end of the tibia (see Figure 47). The data contains these two vectors for every frame (time step) of the video. So the data file contains two columns of vectors that show the history of the position of the femur and tibia throughout the walking cycle.

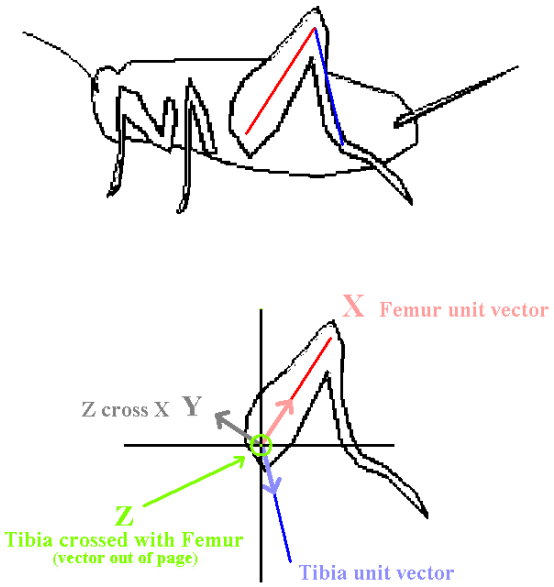

Figure 47. Vector Orientation and Femur Coordinate System

The femur-tibia joint is a simple hinged single degree of freedom joint. Using this fact we established a coordinate system on the femur that puts the femur-tibia joint's excursion in the XY plane of the femur coordinate system. We defined $\mathbf{X}_f$ as the digitized unit vector pointing

from the femur-body joint to the femur-tibia joint. $\mathbf{Z}_f$ was defined by crossing the $\mathbf{X}_f$ vector with a unit vector that points from the tibia-femur joint to the end of the tibia. Finally $\mathbf{Y}_f$ is defined by crossing the $\mathbf{Z}_f$ vector into the $\mathbf{X}_f$ vector. This is now the transformation matrix from the body coordinate to the femur coordinate. This transformation matrix is calculated for each pair of femur tibia vectors for each captured frame (time step) of the high-speed video. There is now a series of transformation matrices from the body coordinate system to the femur coordinate system at a particular time step. By taking the dot product of one time step onto the next time step a coordinate transformation between coordinate system of one time step to the next is calculated. Using this time step n to time step n+1 transformation matrix to calculating the unit vector that does not change from the n step to n+1 step we have the axis of rotation from step n to n+1. We repeat this for every interval between steps and we can produce a plot showing where the axis of rotation of the body-femur joint is through out a crickets walking cycle. If the rear leg is truly a two-degree of freedom leg then the axis of rotation for the body femur joint will not move in either the femur reference frame or the body reference frame.

In practice the digitized data have some error inherited from the digitizing process. To help reduce the effect of these errors the axis of rotation is actually calculated between more separated time steps. This makes the calculation less sensitive to small digitizing errors. The graph in Figure 48 was produced by calculating the axis of rotation from step n to step n+12. This greatly reduced the effect of small errors introduced by the digitization process.

The cricket has many degrees of freedom at the body femur joint. So, as expected, the leg did not show only one axis of rotation, but it did show little variation of the axis of rotation while in stance and swing. The vector's average deviation of 11 degrees away from the average vector. Much larger deviations were present during the transition from one to the other phase. This was most likely due to the loading and unloading of the leg. The important thing was that during stance and swing the leg behaved like a two-degree of freedom leg and that our model could capture this important motion in a very similar manner. So taking an average vector of the axis of rotation of the femur at the femur-body joint we were able to determine the orientation of the axis in both the femurs reference frame and the body reference frame (see graph in Figure 48). Figure 49 shows the cricket like posture of the legs.

9.3 Prototype Cart Design

The prototype cart was constructed with rear legs that closely mimicked those of the insect, in orientation and proportions, but with using only two degrees of freedom. The legs are in a splayed configuration, much like the cricket uses when walking. The cart and leg structure components were machined from Delrin. As with the first prototype leg, the tibia and tarsus were made using stainless steel tubing and music wire. Actuators originated and inserted directly onto structural members of the chassis and legs. This arrangement proved to be cumbersome and resulted in a slightly limited range of motion. At each of the four joints, a single actuator provided extension while an antagonist extension spring produced flexion.

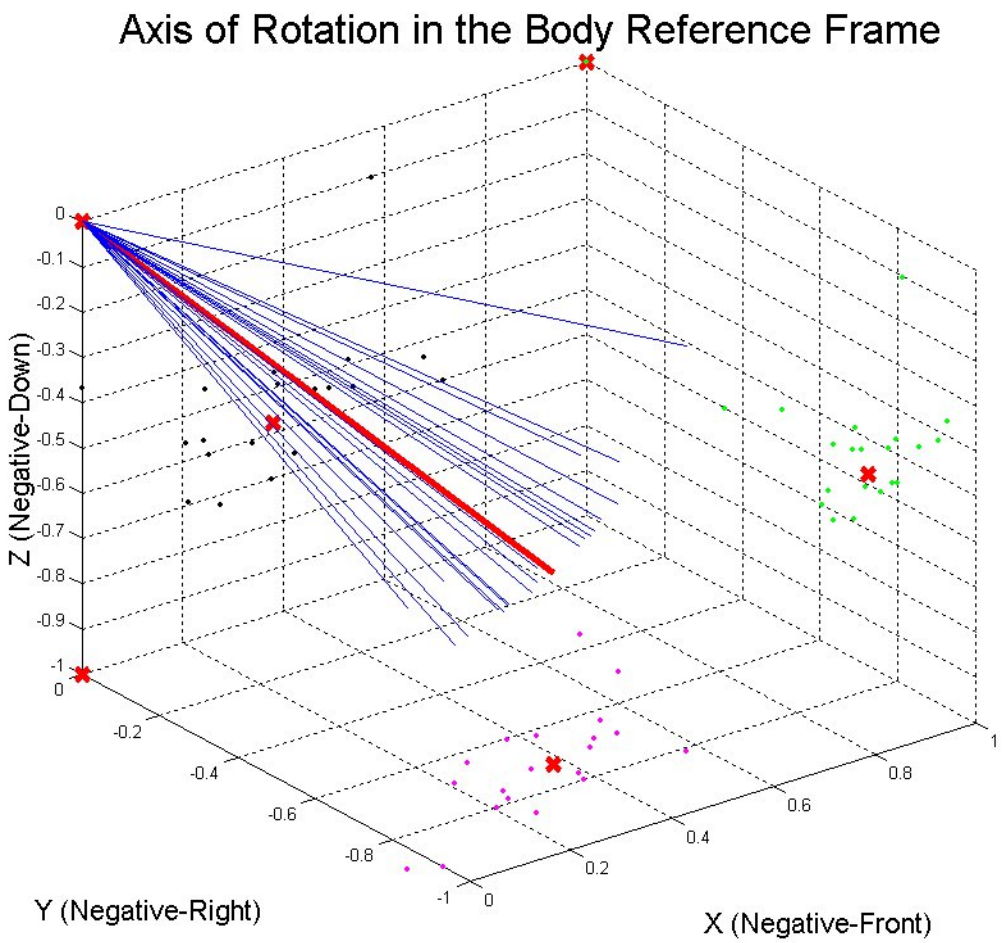

Figure 48. Axis of Rotation in Body Reference Frame. Blue Line Represents Various Positions While in Swing and Stance. The Magenta, Black, and Green Points Represent the Projection of the Vectors Into the Respective Planes XY, XZ,YZ. The Red Line Represents the Average Position of the Axis. The Red "X" Represents the Projection of the End of the Average Vector.

Also, studies of both the cricket and the robot suggested the need for tarsal spines, two relatively large, sharp spines that protrude from the tibia-tarsus joint at the base of the tarsus. On many terrains, forward progress is limited if the spines are not present. Figure 50 shows a cricket launching with and without spines and Figure 51 shows the spines incorporated into the proto-cart's legs.

The two axles for wheels in this early prototype were cannibalized from a Hot Wheels® toy car. The cart needed additional weight to act as payload and to help balance the back-heavy robot. In testing, a 0.5 x 1-inch bolt, which weighs 50 grams, was placed over the wheels. The entire cart weighs 14 grams. Several tests were done using off-board air supplied through a Matrix 3-way valve block that allowed inflation or deflation of the actuators. "Bang-bang" control was used

and there was no attempt to trap air in the actuator. The robot made good forward progress and could easily move its relatively heavy payload.

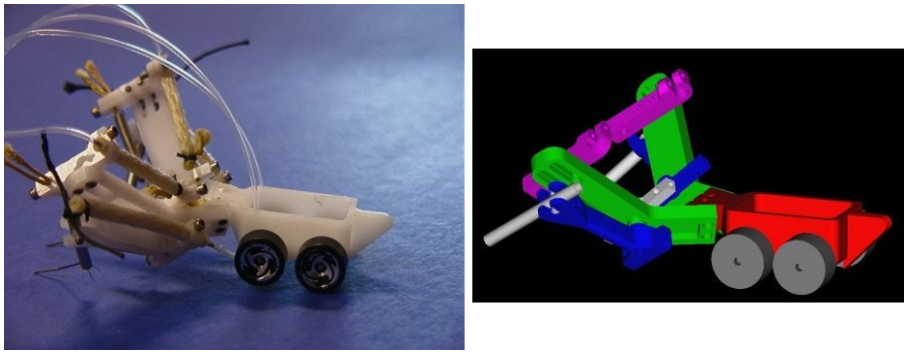

Figure 49. Left: Cricket Cart. Right: CAD Drawing of Cart

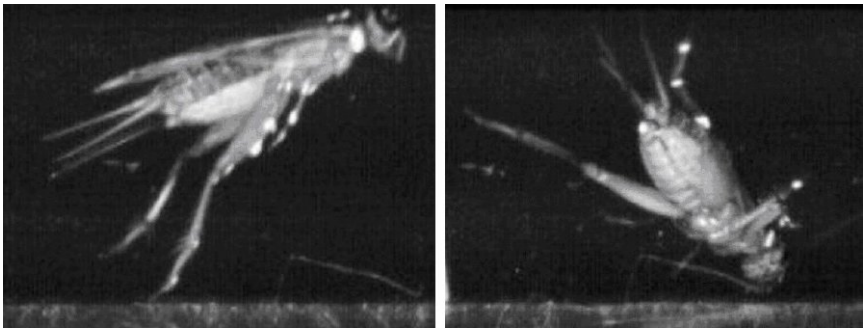

Figure 50. Left: Crocket Jumping With Spines Intact. Right: Cricket Jumping After Spines Removed

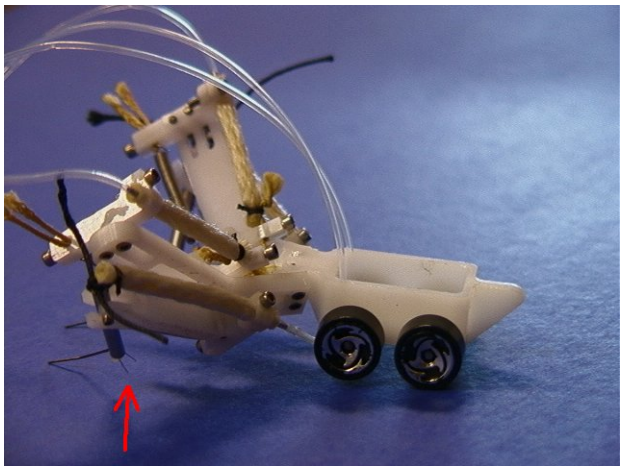

Figure 51. Side of Proto-Cart, Red Arrow Points to the Tarsus Spines

Testing proved that more compliant tubing was needed to supply air to the actuators. The early prototypes used Teflon tubing, which could handle extremely high pressures, was very thin walled, and extremely light but it was too stiff for the robot. The tubing stiffness impeded the robot's locomotion and could stop motion if the umbilical was not supported and moved along with the robot. We also learned that the rigid mounting of the actuator hampered the flexibility and range of motion of the robot's joints. The rigid mount combined with the stiffness of the inflated actuators would bind the joints. A positive outcome was that acceptable locomotion with the reduced degree-of-freedom legs using simple "bang-bang" control was achieved. The biologically-inspired, reduced degree-of-freedom legs performed well and appeared to move similarly to the cricket legs during walking. The legs using off board air and control were able to propel this prototype at about 0.4 in/sec. Greater velocity probably could have been achieved, but the stiff Teflon tubing that supplied the air made this difficult. The vehicle proved the concept, but testing for optimal speed was not done. The fact that the vehicle performed as hoped and expected made this project a success and many lessons involving spring and actuator arrangements and hoses and fittings were learned. Many of these lessons were incorporated into the first attempt to create an autonomous two-legged cricket cart, which is described in the next section.

10. CRICKET CART I

10.1 Introduction

The first autonomous cricket cart pictured in Figure 52 was also the first attempt to integrate all the components of our project to form an autonomous vehicle.

As can be seen in Figure 52, the cricket cart does not have legs that are splayed out like the proto-cart did. The proto-cart showed that we could produce cricket-like walking motion using two degree-of-freedom rear legs. However, this configuration made it difficult to mount all the components in the available space. Therefore, a step back to a more abstract model with more orthogonal joint arrangements was done to facilitate the attempt to make the system autonomous.

10.2 Simulation

A simulation of the cricket cart was written for controller development. We derived the equations of motion for a single leg based on the properties of the first prototype leg. Because the leg was planar, the derivation of the equations of motion was relatively straightforward. We used Lagrange's equation to derive the two DOF leg model, which essentially was a double compound pendulum. What made the simulation interesting was the braided pneumatic actuator model used. This model was taken from [11] and was based on work done by Chou and Hannaford [8].

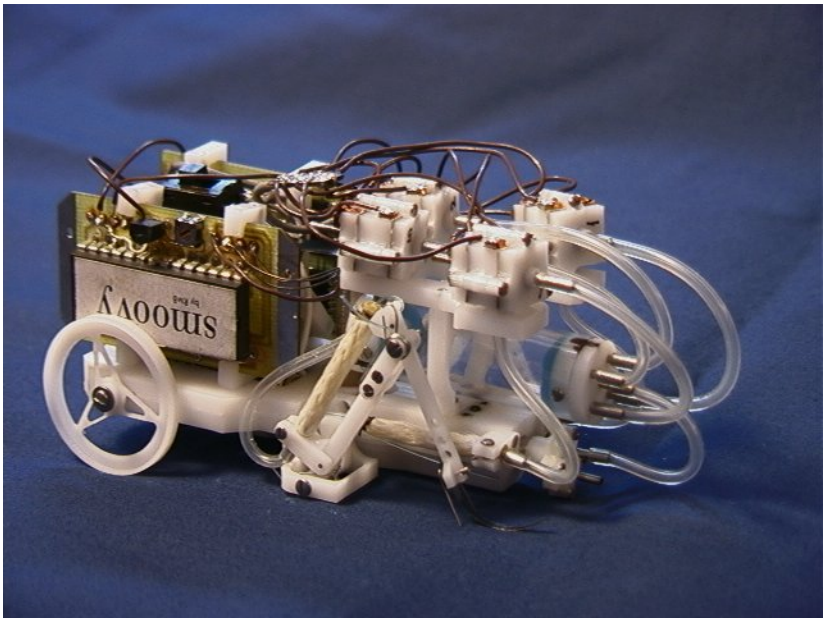

Figure 52. Cricket Cart

For modeling, design and control purposes a fast dynamic simulation of the hybrid robot was developed. The starting point was the cricket model, but it was simplified to be a planar system with just two legs based on the cricket's rear legs. This simulation was used to understand the displacements and forces for the robot, to refine the robot design and to evolve a controller as described in section 10.

The robot model has a pair of two-segment legs, which attach to the body at its center of mass. Each joint is extended by a modeled McKibben actuator [7], and is flexed by a passive linear spring.

Ground contact by the feet is modeled by attaching a virtual spring-damper system in both the x- and y-directions to the foot when it passes below ground level. These virtual springs connect to the surface of the ground at the horizontal position where the foot passes through the ground. A friction model determines if the foot slips. If the foot does not slip because of static friction, ground-model springs are stretched to keep the foot in place. If the foot is found to slip, kinetic friction models the sliding and the attachment points of the ground-model springs are shifted. Stiffness and damping constants are chosen empirically to prevent the foot from penetrating too far into the ground and to provide realistic behavior. The inputs to the simulation from a controller are signals that open and close the modeled valves. The outputs include joint and body motions and ground reaction forces.

We coded the original simulation in C and output the resulting data as a text file in a format compatible with the program X-Animate, which animated the simulated leg. Once the mistakes and bugs were worked out of the equations and actuator model, the simulation was updated to include a body to represent the chassis and a second leg and thus free-body planer motion of the two-legged assembly. A ground model was also implemented. The model was refined and coded in C++ [5]. Visualizer software was developed to illustrate the model (see Figure 53).

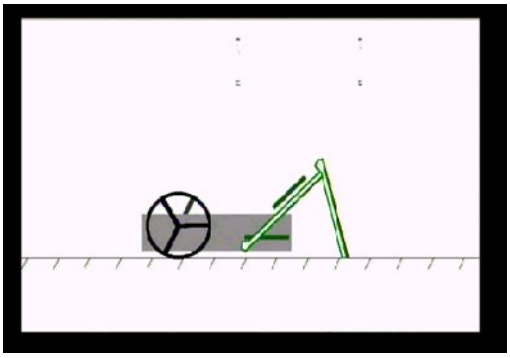

Figure 53. Screen Shot of Visualizer

The simulation provided insight into the function of the two-legged cricket cart. More importantly, it was used with a genetic algorithm to evolve a neural network controller for the robot [12].

10.3 Construction

For the purpose of simplifying the design, the legs were placed in a more orthogonal orientation as compared to the cricket. The gross orientation of the leg retained a cricket-like appearance, with the body-femur joint being near the middle of the robot front to back like the animal and the high femur-tibia joint of the leg grossly similar to that on the animal. The angles calculated for the proto-cart were abandoned because of size constraints and mounting the other components on the robot without raising the center of gravity too high. The rest of the robot's structure was designed in an effort to keep it as small and compact as possible.

The robot was constructed using techniques described in the machining section. The first generation 5mm compressor was integrated into the chassis. The legs used yoke joints. The yoke was on the proximal side of the joint, while the blade was on the distal side. The antagonists to the actuators on these joints were torsional springs, an improvement gleaned from the prototype cart. This made the springs lighter and more compact. Other improvements on the previous design included moving the body femur actuators more inboard and using tendons to aid in the insertion of the actuators on the more distal segments. In this version, the tendons were monofilament line. The tendons were clamped under screw heads, which made their effective length adjustable. To eliminate the changing moment arm of the first prototype leg, constant radius insertions were used. This simplified both the construction of this version and the simulation calculations.

Unlike the prototype leg, the tibia was machined out of Delrin. The tarsus was constructed from spring steel and music wire, creating a better foot for a variety of terrains (see Figure 54). The springiness of the tarsus produced a large, compliant, contact surface, which helped on hard or slippery surfaces. The spines, made from 0.015-inch diameter music wire, would dig into some surfaces again helping with traction on certain terrains.

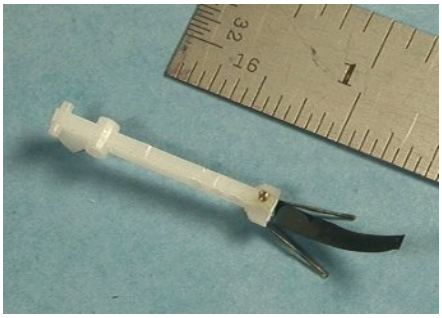

Figure 54. Tibia, Tarsus and Tarsal Spines

The integrated compressor included a motor mounted vertically near the midpoint of the robot that protruded through the bottom of the chassis (Figure 55). The crank, linkage and piston/cylinder were all mounted on the aft underside of the robot and the check valve package was at the aft-most end of the robot. A skid cover across the bottom of the robot protected the compressor components.

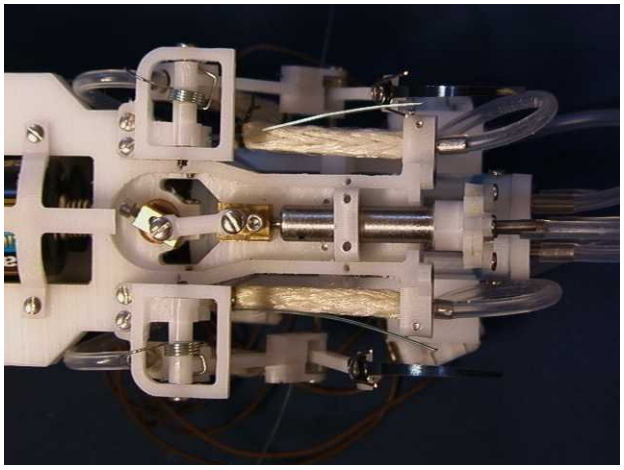

Figure 55. Integrated Compressor

Figure 56 shows the pressure tank/manifold above the compressor, in the rear of the robot. This small, thin-walled plastic cylinder was a pressure reservoir and low-pass filter. It filtered out the 10-20 Hz pulsations from the compressor. The tank was made from a polycarbonate tubing 0.5-inches in diameter with Delrin plugs. One end was ported with five fittings: One inlet from the compressor and four outlets to the valves. Sealing this was a challenge. After much experimentation, RTV sealant was found to work reliably on the polycarbonate and Delrin. The air was distributed from this tank to the four valve packages where it was then plumbed out to the actuators. The batteries were housed in the front of the robot. They are situated in series with their long axis parallel to the long axis of the robot.

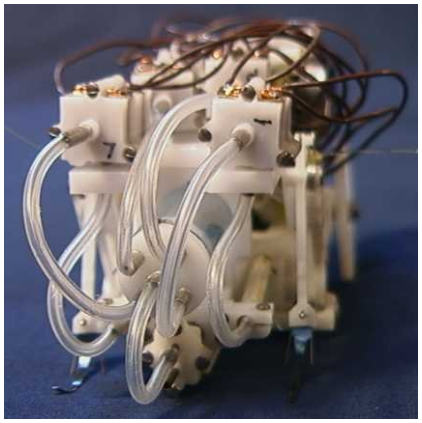

Figure 56. Aft of Robot Top: Valve Packages. Middle: Pressure Manifold. Bottom: Check Valve

On either side of the battery compartment were the two controller boards required to run the robot. On the left side was the Smoovy stepper motor controller, which was required for the brushless stepper motor that ran the compressor. The Smoovy motors were very efficient and had a good torque-to-weight ratio, but their controller was a serious hindrance to the autonomy of the robot. Figure 57 shows the side of the robot where the large controller board is visible. The Smoovy controller was miniaturized as much as possible, but was still very bulky and massive. On the other side of the robot was the PIC controller board. This was a custom built circuit board that incorporated a PIC controller and all the needed circuitry. This board was responsible for power regulation and valve control. Voltage regulation was required because the Smoovy motor controller required 9V, but the battery supply was only 6V. To accommodate this, a step up voltage control circuit was added to the PIC. The PIC also controlled a set of mosfets that supplied the 6V 100mA current to operate the valves.

10.4 Onboard Electronics

Onboard electronics consist of two parts: controller hardware and power source. A PIC micro-controller controls not only the operation of the voltage regulator but also the MEMS valves as shown in Figure 58.

The power source for the robot is a pair of CR-2 3V lithium batteries. The batteries drive the controller boards, compressor motor and valves. The batteries have been tested on a stand-alone compressor and the Smoovy™ motor, which ran for over an hour. The controller and valves reduce this continuous running time to about twenty minutes.

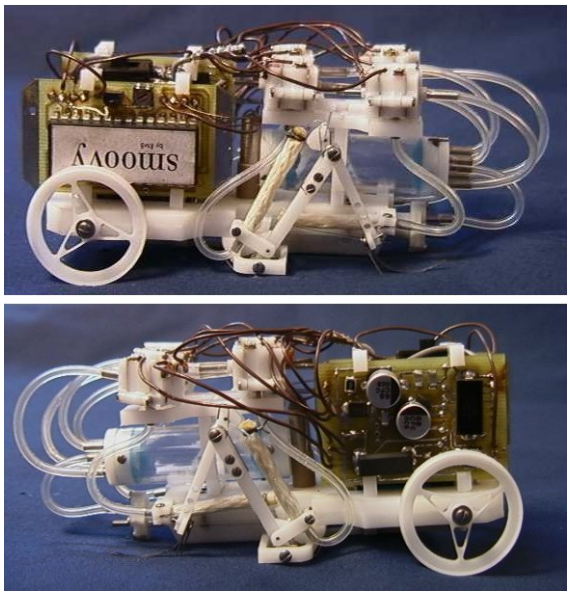

Figure 57. Top: Left Side of Robot Smoovy Controller. Bottom: Right Side Pic Controller

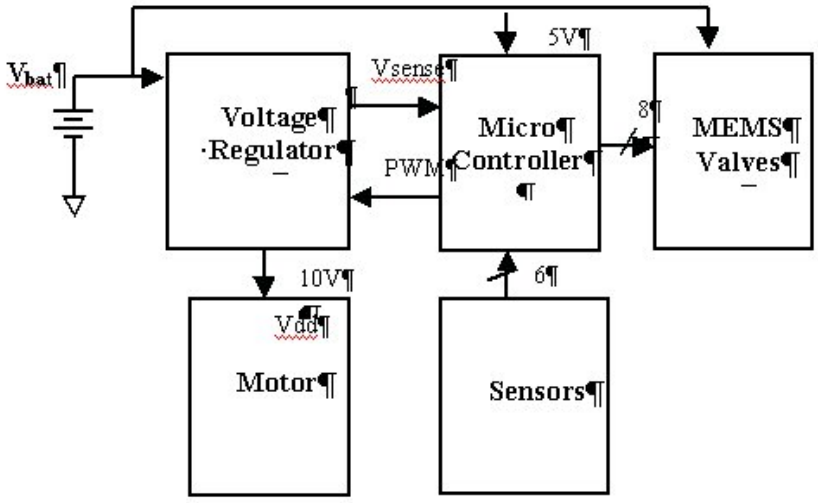

Figure 58. Block Diagram Showing the PIC Microcontroller Controlling the Voltage Regulator and the Eight Valves to Coordinate Locomotion.

The motor operates best at 10 Volts, for which it drains about 160 mA current. Each MEMS valve draws 100 mA current at 5 Volts when it is on. In this application, four valves can be on at the same time. As a result, when the robot draws maximum current, which means the motor is running and four valves are open, the maximum power consumed by the robot is about 3.6 Watts. Two CR-2 3V lithium batteries cells were found to meet the robot's requirements.

Two cells in series and under load can only provide about 5 Volts, but the motor requires 10 Volts. Hence, a switching voltage regulator is used to convert the 5V battery voltage to 10 Volts.

Figure 59 is the schematic of the voltage regulator. The basic operation of this circuit consists of two parts corresponding to the level of gate voltage V_g of transistor M1. When V_g is high, M1 is on, the diode D1 is reverse-biased, and energy is stored in the inductor. When V_g goes low, M1 is off, D1 is forward biased, and the energy stored in the inductor is transferred to the capacitor. The capacitor charges up until the energy balance is reached. V_g is controlled by a Pulse Width Modulation (PWM) signal, whose duty factor can be changed.

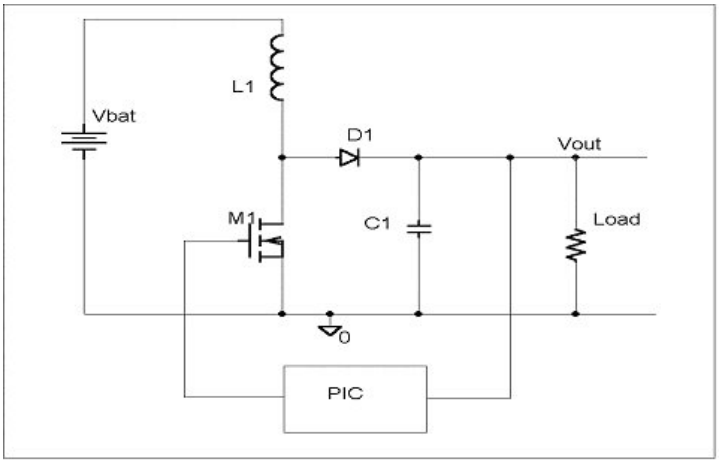

Figure 59. Schematic of Voltage Regulator.

The result of open-loop simulation shows that output voltage (V_{out}) has a linear relationship with the duty factor of the PWM input (DF) for DF < 67%. The gain factor is 10–22 V/DF depending on the number of valves opened. Power efficiency is 87% - 92%, if DF is less than 67%.

Based on the open-loop result, a closed-loop control algorithm has been designed to maintain V_{out} at a desired value. The microcontroller senses V_{out} via its A/D converter channel, and then adjusts the duty factor of its PWM output according to the difference between V_{out} and the desired voltage. If V_{out} is higher than the desired voltage, the PIC reduces the duty factor of the PWM output, and vice versa.

Figure 60 shows the measured behavior of the voltage regulator. V_{bat} is battery voltage, and V_{out} is output from the voltage regulator. During the first 60 ms, the voltage regulator is not activated due to the startup period of the microcontroller oscillator. After the microcontroller starts to provide a PWM output, V_{out} rises from 5 Volts to 10 Volts in 5 ms.

10.5 Controller Software

Two controllers were developed for the robot: a feed-forward scheme using timing, and a feedback scheme using a continuous-time recurrent neural network (CTRNN) in the control loop. The feed-forward controller, programmed on a PIC microcontroller, sends a sequence of pulses to the actuator valves to operate the legs. It ignores feedback signals completely, and depends on the legs reaching their extents of motion to maintain its operating range over time.

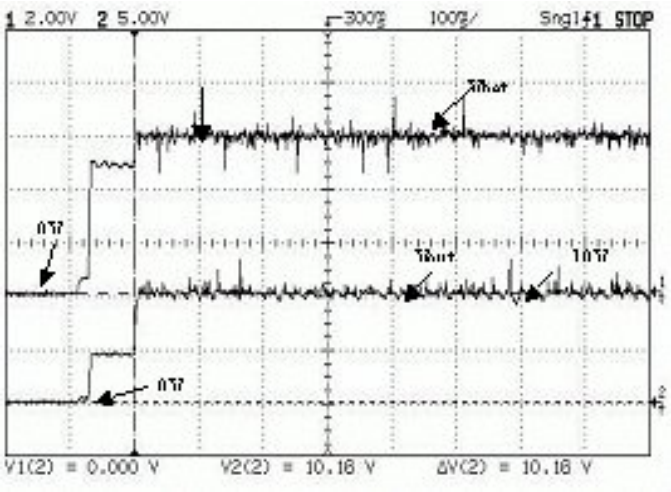

Figure 60. Measured Voltage Regulator Behavior.

The continuous-time recurrent neural network (CTRNN) is governed by the following state equation:

$$\tau_i \dot{y}_i = -y_i + \sum_{j=1}^{N} w_{ji}\sigma\left(g_j \quad (y_j + \theta_j)\right) + I_i \ldots\ldots\ldots\ldots i = 1,\ldots, N \qquad (10)$$

where y is the state of each neuron, τ is its time constant, w_{ji} is the strength of the connection from the j^{th} to the i^{th} neuron, g is a gain, θ is a bias term, $\sigma(x) = 1/(1+e^{-x})$ is the standard logistic activation function (or sigmoid function), and I represents an external input (e.g., from a sensor). States were initialized to small nonzero values, and the circuit equations were integrated using the forward Euler method with an integration step size of 1ms.

The CTRNN-based controller was developed using a genetic algorithm (GA) operating on the robot simulation discussed above to search the multidimensional neuron parameter space – in this case, 61 dimensions – as these parameters are difficult to tune by hand. A GA uses a fitness-function heuristic to guide the search into regions of the search space, which solve the problem most effectively. In our earlier work, the fitness function was trajectory-based, minimizing the mean-square error from a predetermined joint angle trajectory. However, a behavior-based function, wherein a general global behavior is measured and rewarded or penalized, is a far more efficient method of measuring fitness. The fitness function used in this search was the forward progress of the robot at the end of its 10-second trial. To discourage the degenerate solution of extending both legs once and stopping, an incentive was added to encourage oscillatory behavior at the output; the fitness received a bonus for each change in valve state, up to 100% for each of the four actuators.

A real-valued genetic algorithm [30] was used to evolve CTRNN parameters. A population of individuals was maintained, with each individual encoded as a length *M* vector of real numbers. Initially, a random population of vectors was generated. Individuals were selected for reproduction using a linear rank-based method. A specified elitist fraction of top individuals in the old population were simply copied to the new one. The remaining children were generated by either mutation or crossover with an adjustable crossover probability. A selected parent was

mutated by adding to it a random displacement vector whose direction was uniformly distributed on the *M*-dimensional hypersphere and whose magnitude was a zero-mean Gaussian random variable. A neuron's time constant, bias, and output weights were treated as a module during crossover. The search parameters in the range ±1 were mapped linearly into CTRNN parameters with the following ranges: connection weights ∈ [-8,8], biases ∈ [-4,4], and time constants ∈ [0.01,0.1]. All neuron gains were set to unity and were not evolvable.

The neural net architecture (Figure 61) consists of 16 symmetrically arranged neurons; that is, all of the interconnections and neuron parameters were mirrored exactly from one half, which controlled the left side of the robot, to the other half. The first layer of neurons receives inputs from sensors mounted on the robot. A foot-contact switch provides an input value, which is either zero, if open, or equal to a value evolved as a GA parameter, if closed. The joint limit switches act in pairs for each joint: if a joint reaches its flexion joint limit, an evolved parameter value is supplied to that input neuron; if the joint reaches the extension limit, the negative of that parameter is supplied as input; and if neither limit is reached, an input of zero is supplied.

The input neuron layer has feed-forward connections to the layer of "interneurons" (neurons with no external connections), which consists of three neurons on each side, and whose neurons are fully interconnected with each other and themselves. The three interneurons on each side have feedforward connections to the third, or output, layer of neurons. Each neuron – two per side – controls the valves for one actuator. As the neurons are based around the sigmoid function, their outputs always range from zero to one. Thresholds were evolved to determine what levels would indicate valve openings and closings. Below the lower threshold, the outlet valve opens; above the upper threshold, the inlet valve opens; and in between, both valves stay closed.

The robot used a Microchip PIC 18C252 control its motion as well as the compressor supply voltage. Although a manually designed feed-forward controller was ultimately installed on the robot for controlling motion, work was done to investigate the effects of loss of computational precision on the operation of the neural network.

The robot simulation was modified to contain a fixed-point arithmetic implementation of the CTRNN. Various neuron parameters were stored as 16-bit fixed-point numbers, and the calculated neuron states were stored with 32-bits of precision. A neural network evolved under double-precision floating-point arithmetic was converted to work with the fixed-point arithmetic, and was used to run the simulation in real-time. While there was a slight difference in step frequency between the floating-point and fixed-point behaviors (Figure 62) there were no other appreciable differences between them. In addition, a conversion routine was written to convert neural network parameters to a set of constants for direct use in PIC assembly-language routines, to allow for direct implementation of a neural network on the PIC.

10.6 Results

The assembled robot weighed a total of 94 grams. The wires and hoses weighed 22 grams. The two circuit boards together weighed 30 grams, and the batteries were another 28 grams. The remaining 14 grams of the robot encompassed the chassis, legs, wheels and actuators. The robot never achieved power autonomy, but all of its components were functional and it only required external air. The compressor was able to generate sufficient pressure, but could not provide the

required flow. Leaks were a problem and detecting them was more difficult than repairing them. Even an almost undetectably small leak in a system with such a small volume of compressed air was a serious waste of power.

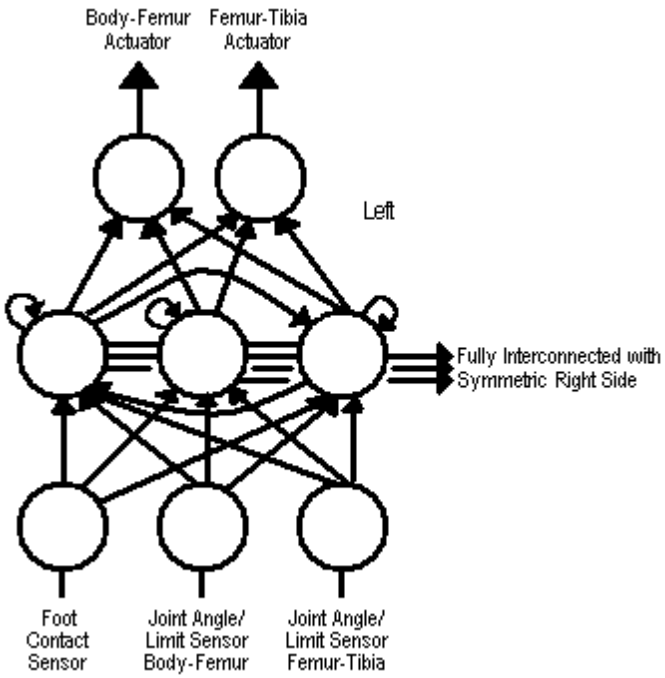

Figure 61. Fully Connected, Continuous Time Recurrent Neural Network for Control of Locomotion

Many things were learned from the first generation robot. Monofilament was much too stiff for use as tendons. Its stiffness actually hinders joint flexion. The robot's construction was overly complicated for its scale. The joints were over-engineered. The fewer air connections, the better. Since leaks were a serious problem, the fewer the number of connections the better. Finally, the Smoovy motor controller was too large and heavy.

The robot's speed using on-board power to operate the controllers and valves, but having air supplied from off board, was about 0.011 body lengths per second. This slow speed was due to a conservative program in the controller. With latter tests and a new controller program, the robot achieved about twice the speed, or 0.022 body lengths per second. Due to its underpowered legs and poor flow through the onboard valves, the robot was never tested for turning radius. The robot had difficulty just lifting its abdomen off the ground. The real success of the robot was the nearly complete integration of the components. Although the robot never functioned autonomously, all needed components were present and functioning. This promising integration and apparent shortcomings prompted a transition to the next generation of the cricket cart. In the next version we worked to fix the shortcomings and refine the design.

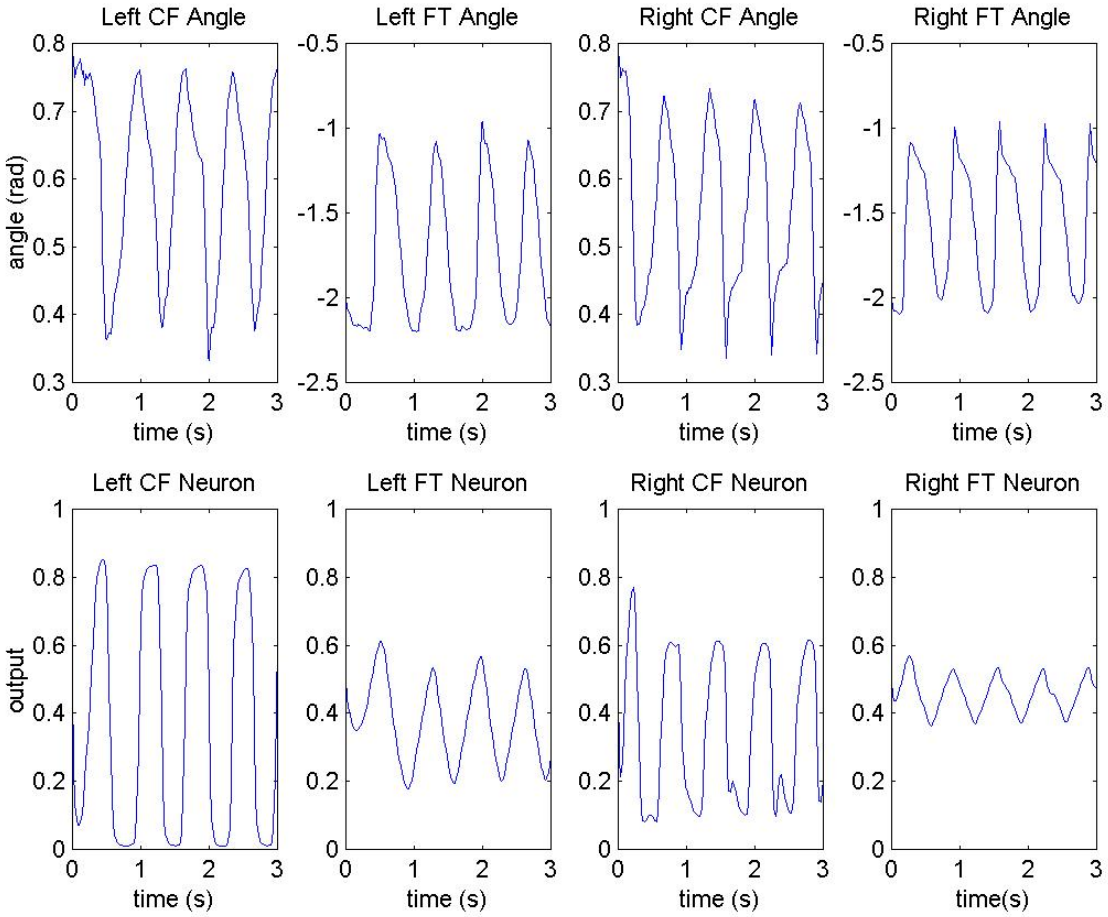

Figure 62. Output of Neural Network. Top: Floating Point Behaviors. Bottom: Fixed-Point Results.

11. CRICKET CART II

The second generation cricket cart (Figure 63) incorporated many improvements over the first version. The legs were greatly simplified using less fasteners and simpler construction. Rather than the yoke joint, the axle diameter was increased and the axles were made cantilevered. The axle diameter was increased to allow a 1-72 screw to pass through the axles. This provided better axle bearings and provided the strength needed to support the cantilever axles. It reduced the total number of screws in the leg from 11 to 8 per leg and the number of machined parts from 6 to 4 (Figure 64).

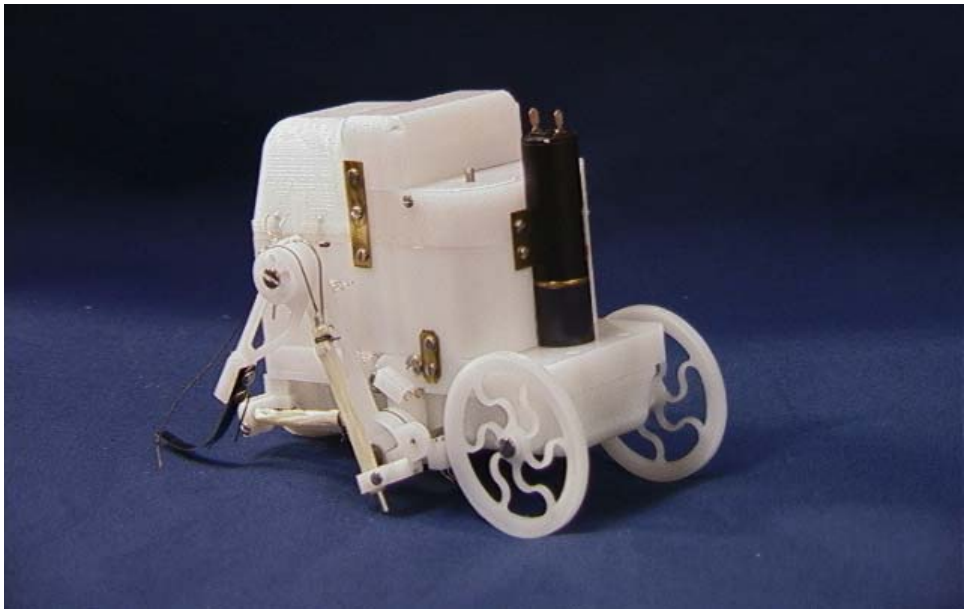

Figure 63. Cricket Cart II

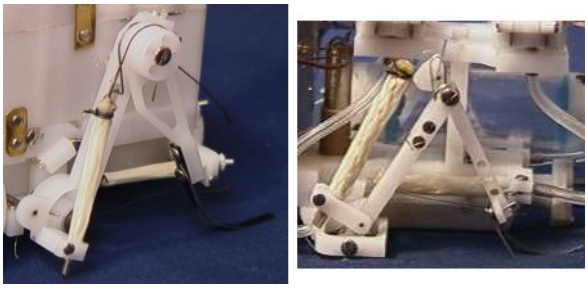

Figure 64. Right: New Leg. Left: Old Leg

The new actuators and their supple silk tendons were attached to much wider, simpler, constant radius moment arms that increased their reliability and reduced the precision needed in their mounting. Again, the tendon attachments were achieved using a screw that pinched that tendon, allowing for quick and easy adjustments of their effective lengths.

The legs were also enlarged. After all the work that was done on the micro actuators, a practical size that functioned well had been developed. It was more practical to scale the leg up to a size appropriate for the new actuators rather than redesigning the actuators again at this stage of the project.

As in the first generation, each joint used torsional springs to act as antagonists to the braided actuators. But in the second generation, torsional springs were custom-made from music wire. Due to limitations in the stiffness and orientation of the ends of commercially available springs, it was decided to fabricate the springs. Custom springs could have ends oriented and bent into more convenient shapes (Figure 65). Since the excursions were relatively small, there was no yielding the springs.

Figure 65. Custom Springs

Another improvement was that more features were machined into the second generation chassis to reduce the part count and simplify the assembly task. The second generation was also better contained, keeping hoses and wires under covers as much as possible to keep them from catching or snagging on their surroundings.

The compressor built into this robot was the larger, third generation Maxon gear motor-driven compressor (Figure 66). The mounting of the motor and transmission was made simpler and easier with screws that went directly into the transmission housing. The cylinder mount was adjustable to allow easy tuning of the compressor's top dead position relative to the check valves. In this version, the compressor ran the entire length of the robot, with the motor in the very front of the robot. The new skid plate to protect the compressor also supported the wheels and provided a better snag-free bottom to the robot.

To eliminate many of the valve connections, the valve packages were machined directly into the side of the pressure reservoir, which made for a more easily sealed valve package. However, this design did require one part to have 16 00-90 blind screw holes to be drilled and tapped. The finished valve manifold package required a total of 32 00-90 screws and 8 0-80 screws (see Figure 67). This complexity of design helped eliminate 8 fitting and 16 fittings to Delrin or fitting to hose connections. This Cricket Cart II had only five hoses where the cricket cart one had 9 hoses. The entire package was machined from Delrin and the tank was sealed in a similar manner to the compressor's check valve package, using latex cast into channels to form a custom gasket.

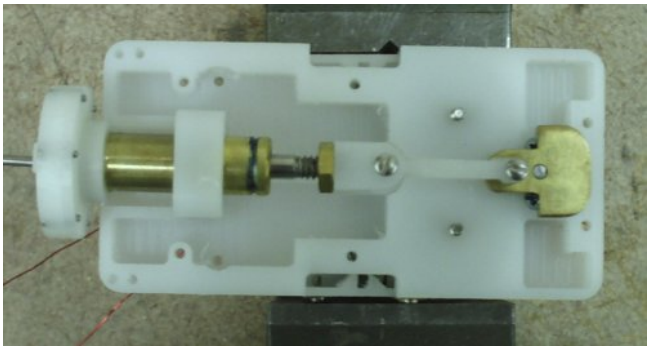

Figure 66. Integrated Maxon Compressor

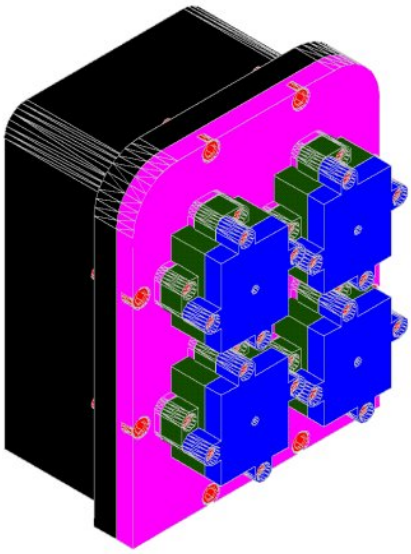

Figure 67. Manifold with Integrated Valve Packages

With this design, the PIC controller board could be made much smaller. The extra circuitry for power regulation is no longer required since the Smoovy motor controller was not being used. This 2nd generation controller now had input and output channels. As another improvement, the robot was simpler and more self-contained, with more internal connections and less wires and hoses. The batteries were placed in a vertical orientation just behind the motor. The controller board was mounted behind that. This made battery changes quicker and easier, requiring the removal of only three screws and the pulling of the batteries through the top of the robot.

The wheels were machined with flexible curved spokes to provide some suspension to the front of the robot (see Figure 68). By making the spokes long and curved some movement between hub and rim would be allowed. It was planned that this "suspension" would help give the wheels some compliance to help climb over obstacles. It did not work as well as hoped because the wheels remained too stiff.

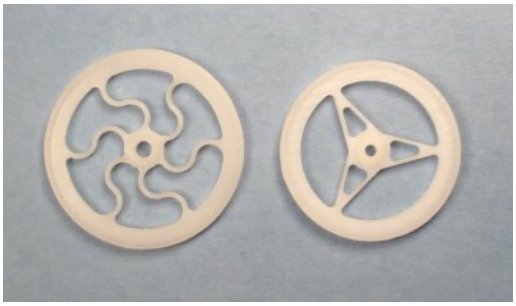

Figure 68. Right: Cricket Cart II Wheel. Left: Cricket Cart I Wheel

Unfortunately, the 2nd generation MEMS valves were not fabricated in sufficient quantity for the second generation cricket cart. Despite this the robot demonstrated a significant improvement in performance over its predecessor. The robot, during testing using off board air and valves, achieved forward velocities of 0.175 body lengths per second, which is over seven times faster than Cricket Cart I. The robot has a turning radius of about 1.23 body lengths. Some of the credit for the increased performance was due to using off-board valves that had better flow characteristic than the MEMS valves. The improved design of the legs and actuators also made a big difference. Where Cricket Cart I could barely support its aft end, Cricket Cart II could easily support itself and was able to walk while supporting this weight.

12. SIX-LEGGED CRICKET

12.1 Introduction

The purpose of the six-legged version of the robot was to test the abilities of a robot using all six legs at the scale desired for this project (Figure 69). It was also the next step towards the ultimate goal of the project, to develop a 2-inch long, self-contained six-legged robot. It was also a step forward toward the cricket's design. For expediency, Cricket Carts I & II had simplified rear legs and wheels in the front. This new robot has six legs, the designs of which are loosely based on the kinematics of the cricket. The entire robot has six legs, sixteen joints, but only eight independent degrees of freedom. Many of the joints are mechanically coupled or co-actuated in some way.

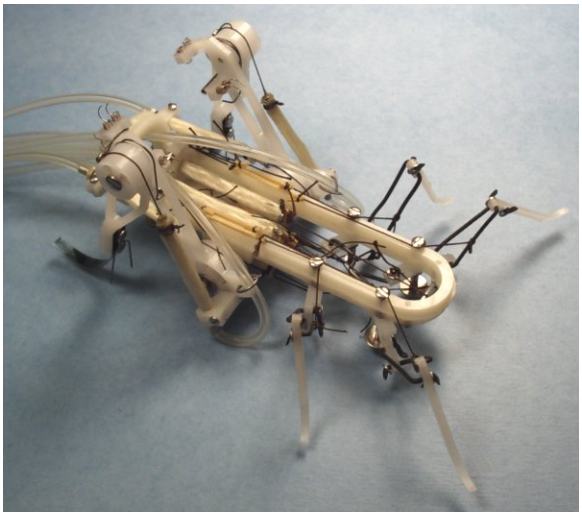

Figure 69. Six-legged Cricket Robot

12.2 Front and Middle Legs

The legs are designed to have specific functions much like those in the cricket. The front and middle legs are similar in construction but have different functions. They were constructed with

the coxa of the leg machined from Delrin. The two pieces for the femur are fabricated from annealed steel wire. The tibia and tarsus are machined as one piece, also from Delrin. The front and middle leg's body-coxa joint rotates around a vertical axis. This joint produces the forward-aft motion of the front and middle legs. To reduce actuation, the body-coxa joint of a front leg is coupled by a linkage (highlighted in Figure 70) to the same joint of the middle leg on the opposite side of the robot. The actuator on this joint when activated produces forward-to-aft motion. This actuator's antagonist is an elastic element, which returns the legs aft-to-fore.

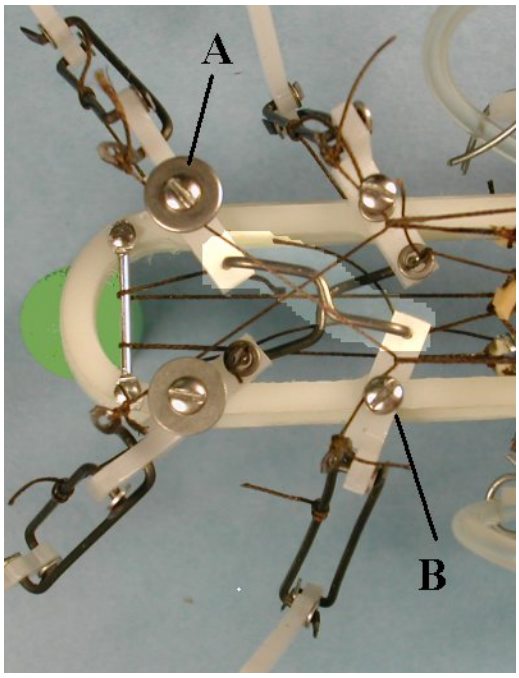

Figure 70. Front Legs: A: Front Leg Body-Coxa Joint. B: Middle Leg Body Coxa Joint. The Interconnecting Link in the Highlighted Area Connects the Two Coxas

The coxa-femur and femur-tibia joints are pairs of joints in a four bar mechanism. The parts can be seen in Figure 71. If the coxa is thought of as the ground link then the output link is the tibia. The two coupler links make up the "femur." The actuator attaches to a moment arm that is part of the upper femur coupler linkage. The actuator is located in the abdomen (Figure 72) of the robot and attaches to the femur linkage via a silk tendon. The tendon is guided by means of pulleys around a lower extension of the body-coxa joint's axle as seen in Figure 70 where the labels point to the lower extensions of the joints. The antagonistic elastic element attaches on the upper femur linkage as seen also in Figure 72 and is also located in the abdomen of the robot inserting along a silk tendon by means of pulleys around the upper body-coxa joint axle extensions. By running the tendon around the body-coxa joint axle, the torque applied to the body-coxa joint is minimized. The coxa-femur and femur-tibia joints are kinematically coupled. These outer two joints of the front leg and its opposite middle leg are co-activated by a single actuator that inserts on both femurs. This results in a paired front and opposite side middle leg having a total of six joints but only two degree of freedom total. One actuator moves the legs for and aft and one other actuator moves the legs from stance to swing. In this way the robot can

move its front and middle legs as needed for a tripod gait. Six-legged insects commonly use the tripod gait for fast locomotion. This gait puts three legs on the ground in stance while the other three legs are in the swing phase. The front and rear legs on one side of the body coupled with the middle legs on the other side will support the body while the other tripod is in the swing phase. By alternating these tripods of legs a tripod gait allows the animal a very quick stable locomotive gait.

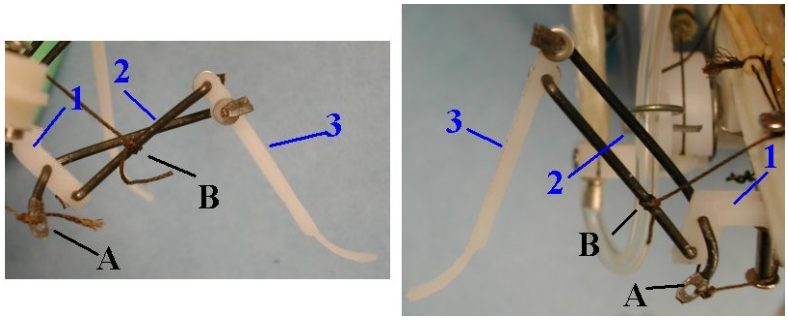

Figure 71. Front legs: A: Denotes Actuator Insertion. B: Denotes Antagonistic Elastic Elements Insertion; 1-Coxa, 2-Femur Links, 3-Tibia/Tarsus

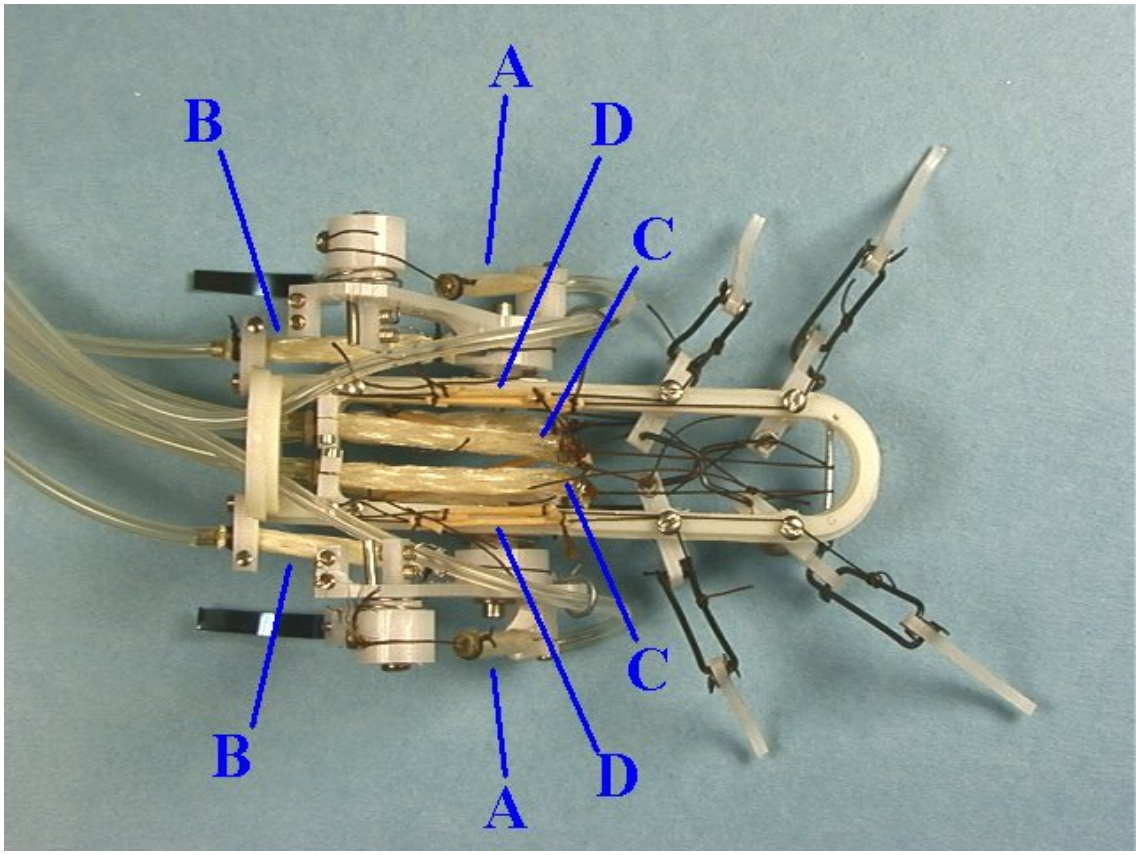

Figure 72. A: Rear Femur Tibia Actuators, B: Rear Body-Femur Actuators, C: Body-Coxa Actuators for Front/Middle Legs (Co-Actuation), Behind C: Are the Actuators for

Front/Middle Leg Extensions Extension (Co-Actuation And Couple Joints) D: Elastic Antagonist for Front and Middle Leg's Flexion, Behind D on the Other Side of the Frame: Similar Elastic Element for the Body-Coxa Joint of the Front and Middle Legs

Although the front and middle legs were constructed and actuated in similar manners they performed different functions (Figure 73). The front legs were designed to aid with climbing. The four-bar mechanism that couples the outer two joints causes the front legs to reach high during the swing phase, allowing them to step up onto obstacles. The drawback of this design is that the front leg cannot carry as much weight as the middle leg can. During a tripod gate, the rear leg on the same side of the body will be in phase with this leg and support for this side of the robot will be shared between the front and middle leg.

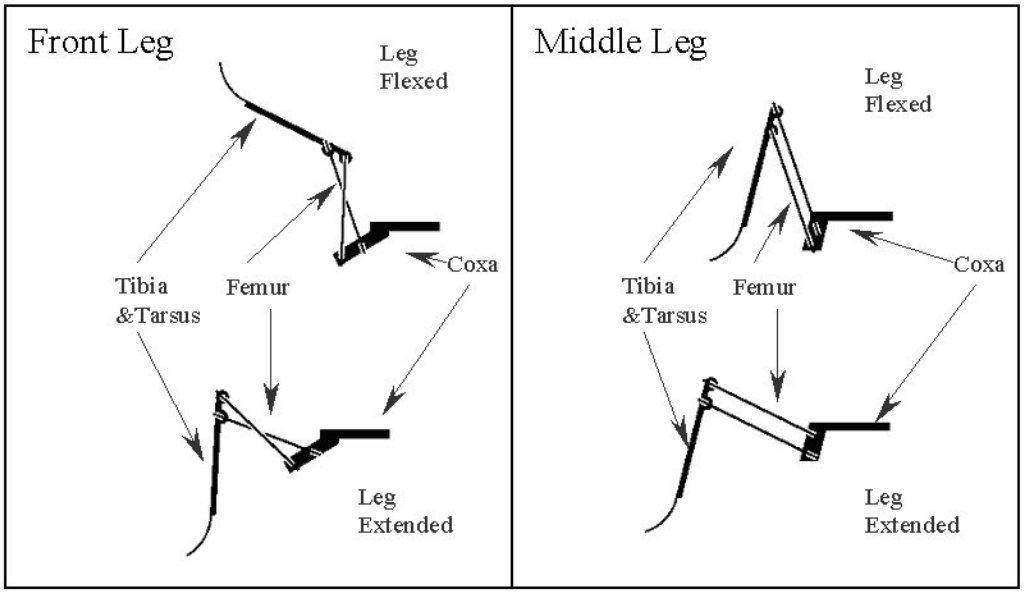

Figure 73. Diagrams Showing the Relative Motion of the Front and Middle Legs

The middle leg was designed to be relatively strong and able to lift half the weight of the robot. Since the robot will use a tripod gait as its primary mode of locomotion, the middle leg must be able to support half or more of the robot's mass since the front and rear legs on that same side of the robot are out of phase with this leg. The leg's design gives it a larger mechanical advantage than the front leg, but it cannot lift as high off the ground during its swing phase.

12.3 Rear Legs

The rear legs are the same design as the ones on the second-generation cricket cart. These simple two-jointed, two degree of freedom planar legs are very powerful and provide much of the forward thrust of the robot. As seen in Figure 74 the actuators that operate the femur-tibia joint of the rear legs are the only actuators on the robot that are not located in the body of the robot.

These actuators are mounted along the femur. Their origins are on the femur near the body-femur joint and their insertion point are on the tibia side of femur-tibia joint. The body-femur joint actuator's origin is at the back of the abdomen, next to all the actuators for the front legs and its insertion is on the femur side of the body-femur joint.

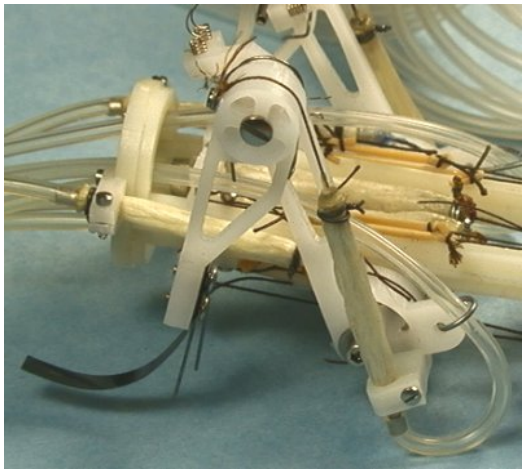

Figure 74. Rear Leg of Six-Legged Robot

The rear legs provided most of the thrust for the robot. Thus, the design of the tarsus on this leg was very important. The tarsus is made of two pieces as seen in Figure 75. One is a piece of spring steel shaped roughly like the cricket's tarsus. This provides a flexible foot to contact and comply with the ground. Also included in the rear leg tarsus is a pair of tarsal spines that were made from 0.025 inch diameter music wire. These are attached to the end of the tibias with 0-80 machine screws.

Figure 75. Tarsus with Spines

12.4 Chassis

The chassis was machined from ABS plastic. The ABS was preferred over Delrin to lighten the robot. The first and second-generation cricket carts were machined from Delrin. Delrin, although more easily machined and tougher, was heavier than ABS, which has a higher modulus and lower density. The ABS also doesn't hold threads as well as the Delrin. This caused minor problems in the assembly of the chassis.

A cover could be put in place to protect the front leg actuators and to keep the linkage on the bottom of the robot from interfering with the terrain and surroundings.

Control of the activation of the actuators was done through a pair of Matrix valve blocks. One block provided the eight necessary inlet valves and the other eight outlet valves. The 2-way valves were paired, producing three-way valves. With a pair of 2-way valves, there are four possible arrangements: 1) both can be opened, allowing high-pressure air to escape directly to the atmosphere; 2) both can be closed, holding whatever pressure is present in the actuator; 3) exhaust could be closed with the inlet open, opening the actuator to high-pressure air; and 4) inlet could be closed with the exhaust open, exhausting the pressure in the actuator to the atmosphere. Only two of the four possibilities stated were used in the operation of this robot. This was done to stay with in the limitations of the valves used on the autonomous version of the cricket cart. Bang-bang control of the valves was used. The control scheme was generated to give the desired tripod gait and a hopping gate.

The tripod gait involves using the six legs in two alternating tripods. Each tripod consists of the front and rear legs from one side of the body and the middle leg front the opposite side. By alternating stance and swing between the tripods, locomotion was accomplished. Because the six-legged cricket robot uses fewer DOFs, the various phases for walking were easy to define. To stand on the first tripod of legs, the body femur joint of the rear leg and the leg extensor for the front and middle legs were activated at the same time (these actuators will be referred to as the "stance actuators"). This is demonstrated in Figure 76, where the robot is relaxed, and in Figure 77, where the robot is standing on the first tripod of legs.

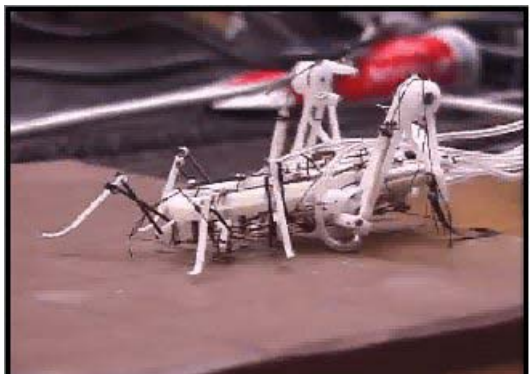

Figure 76. Robot with All Actuators Relaxed

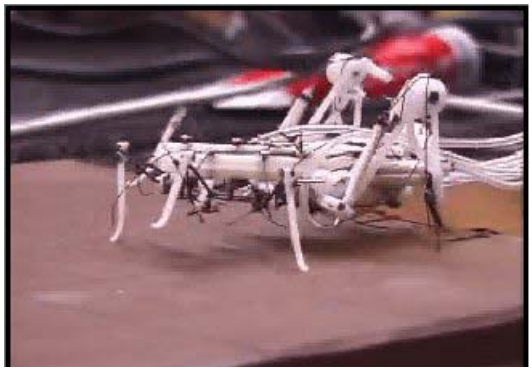

Figure 77. Robot Standing. The Far Front and Rear Legs and the Near Middle Leg Are in Stance.

The legs then propel the robot forward by activating the femur-tibia joint of the rear leg along with the body-coxa actuator of the front and middle legs (these actuators will be referred to as the "step actuators"). Figure 78 shows the robot after a step forward has been taken

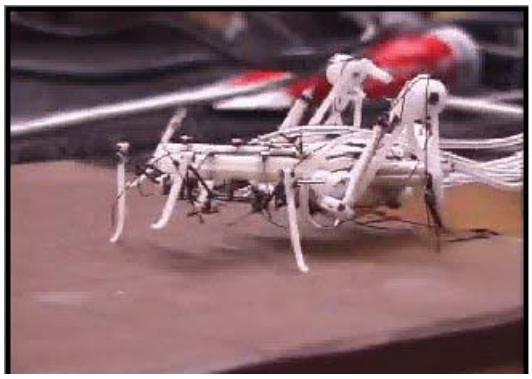

Figure 78. The Robot After Taking a Step Forward

Now the transition from the first tripod to the second tripod can begin, during which the second tripod will move to support the body with the goal of allowing the first tripod to swing forward. Thus for a brief moment, all six legs are in stance (see Figure 79). The activation of the second tripod is a phase-shifted copy of commands for the first tripod.

To complete the transition, the first tripod relaxes its stance actuators lifting its legs off the ground. Then simultaneously the step actuator for the first tripod is relaxed while the step actuators for the second are activated. This allows the first tripod to swing forward while the second tripod propels the body forward. Again a transition is made from the second tripod back to the first. This pattern is repeated as long as desired.

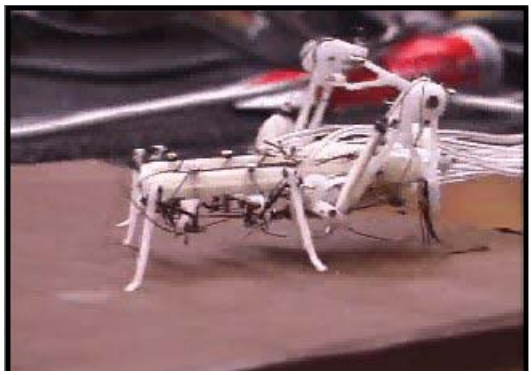

Figure 79. The Robot in Transition With All Legs on the Ground

A lunge was performed during the testing of the robot. This was done by firing all the stance actuators for all the legs and then quickly firing all the step actuators, thrusting the body forward, and then relaxing all the actuators at the end of this motion. This produced a "stiff" looking hop. And although not an efficient mode of locomotion it did show the fast response of the actuators and valves.

The performance of the robot using off board air was surprisingly robust. When lunging, the robot could move forward rapidly about one inch with a single surge of all its legs. Note that these maneuvers included all the inertia of its relatively massive umbilical. When walking, the robot achieved straight-line velocities of about 0.5 body length per second; this is almost three times the speed of the Cricket Cart II. By dragging one of the rear legs and running the rest of the legs normally, we were able to achieve a turning radius of approximately one body length.

13. CONCLUSIONS

The ultimate goal of producing a fully autonomous 2 cubic inch robot has not yet been achieved. However the project has produced several promising technologies, which make an autonomous 2-cubic-inch robot feasible.

Figure 80 is a conceptual drawing we made of the robot during the early phases of this project. Although a robot like this one has never been built, most of the components in this figure have been demonstrated in one or more of the robots described herein. The arrangement of the components in the cricket cart is similar to the drawing and the legs are similar to those on the six-legged robot.

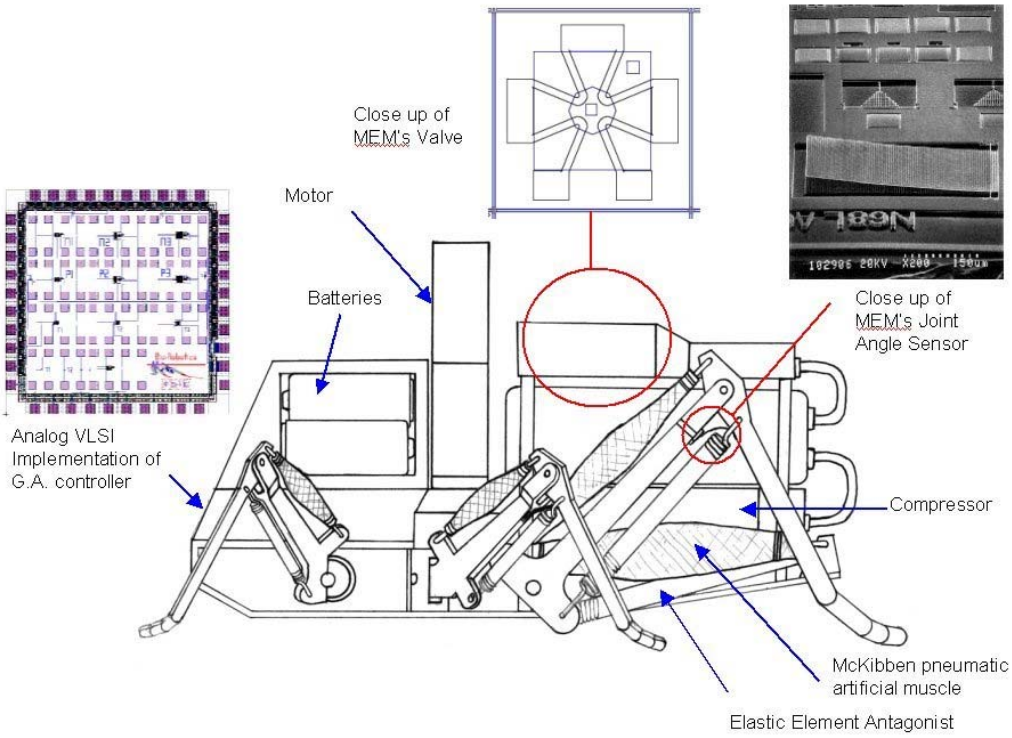

Figure 80. Early Concept Drawing of the Cricket Robot

13.1 Specific Lessons and Possible Improvements

We have developed a very successful series of small compressors. With a minimal amount of fine-tuning, a capable, high-pressure micro compressor could be mass-produced. With modern plastic molding techniques, the check valves could be redesigned for mass production, better performance, and longer life than the prototypes made for the compressor described in this report.

As successful as the compressor is, its flow rate needs to be increased. At the time this document was being written, Maxon released a metal-gear version of the transmission used with the Maxon motor. This improvement alone could possibly increase the flow of the compressor by 50-100%. Another improvement would be to switch from a crank and slider mechanism to a cam-driven compressor. Since the force curve is known, a cam could be designed to lower the maximum torque and increase the minimum torques. By flattening the torque curve, the compressor could be made even more efficient.

Delrin was an excellent proto-typing material but improvement to the design could be achieved by changing to another material for many parts of the robot's structure. Also since the robot was designed to be disassembled and reassembled many times, some performance was lost to facilitate this. If engineered to be disposable, many of the components could be designed to snap together. This would reduce the cost, weight, and complexity of the robot.

Future work would include a semi closed pneumatic system to help overcome the initial pressure problem with the actuators. If a low-pressure reservoir was installed that was at a pressure just below the pressure needed to activate the actuators, the high-pressure reservoir's pressure could be raised by an amount equal to the activation pressure. The time to fill actuators to the activation pressure could be greatly reduced and efficiency could be improved.

The actuators were fairly successful but making actuators with lower initial pressure would improve the system. This would require higher quality material for the bladder. Commercially made tubing may be a better solution due to quality control issues. Another thing that would greatly improve the reliability of the actuators would be to implement some type of molded ends. This would reduce stress concentrations and make the attachment point of the actuator more functional.

Ultimately it was desired to have the autonomous robot jump up stairs and although it would probably be possible, the expenditure of energy for the robot would greatly reduce the life expectancy of the robot. Power storage is still a step behind many of the other technologies.

True autonomy probably could be achieved if all technology had been brought together at the right time. For example, the fabrication of the 2nd generation valves lagged the other components. The MEMS fabrication houses had difficulty making some of the components correctly.

Sensors are another area that needs more work. The MEMS joint angle sensors (Volume 2) were never ready for implementation. Some simple joint limit sensors were incorporated into the design of the second generation cricket cart but where never tested extensively and never used in the controller.

For robot construction, especially the small front and middle legs of the six-legged cricket it would be beneficial to use living joints. By combining material with different properties and casting them together, parts can be molded that have a variety of properties. So you can create one part that will have stiff sections and a flexible section. This would be a great way to create flexible living joints in a monolithic front or middle leg assembly. By picking the correct material, the antagonistic element could be incorporated into the joint simplifying the construction even more.

13.2 Future Work

Many of the technologies that have been developed as part of this project can have uses in applications other than the vehicles discussed here. The actuators could be used in a variety of applications where their high force to weight ratio gives them some advantages over other pneumatic actuators. The compressor also has a wide variety of uses in applications that may or may not have anything to do with autonomous robots. Along with the compressor, the MEMS valves are another technology that can have many uses in other fields.

The robots themselves have advanced greatly since the start of the project. Many lessons have been learned from these vehicles. An autonomous micro vehicle could be achieved in a matter of a year or two. Mission times would still be short due to the low power density of batteries.

Until we can store more energy in a robot this small their missions will have to be short or have dormant periods during the mission.

The possible applications for micro robots are many and include tasks that are too small or are in locations too small for humans, and as the technology advances, cheap and easily deployable mobile surveillance systems are a possibility. There are many applications for small robotic vehicles and as new vehicles are developed, new applications will arise.

14. REFERENCES

[1] Adachi, H.; Koyachi, N.; Arai, T.; Shimiza, A.; Nogami, Y., Mechanism and control of a leg-wheel hybrid mobile robot, *Intelligent Robots and Systems,* 1999, IROS '99. Proceedings. 1999 IEEE/RSJ International Conference on, Vol.3, 1999, Pages: 1792-1797 vol.3

[2] Bachmann, R.J., A Cockroach-Like Hexapod Robot for Running and Climbing, M.S. Thesis, Case Western Reserve University, Cleveland, OH, 2000

[3] Beer, R.D., Chiel, H.J., Sterling, L.S., Heterogeneous Neural Networks for Adaptive Behavior in Dynamic Environments, Advances in Neural Information Processing Systems, D.S. Touretzky(ed.), Morgan Kaufmann, San Mateo, CA,1989, Pages: 577-585

[4] Bererton, C., Navarro-Serment, L.E., Grabowski, R., Paredis, C.J.J., Khosla, P.K., "Millibots: Small Distributed Robots for Surveillance and Mapping". Government Microcircuit Applications Conference, 20-23 March 2000.

[5] Birch, M.C.; Quinn, R.D.; Hahm, G.; Phillips, S.M.; Drennan, B.; Beer, R.D.; Xinyu Yu; Garverick, S.L.; Laksanacharoen, S.; Pollack, A.J.; Ritzmann, R.E., A miniature hybrid robot propelled by legs, *Intelligent Robots and Systems,* 2001. Proceedings. 2001 IEEE/RSJ International Conference on, Vol.2, 2001, Pages: 845- 851 vol.2

[6] Caprari, G.; Arras, K.O.; Siegwart, R., The autonomous miniature robot alice: from prototypes to applications, *Intelligent Robots and Systems,* (IROS 2000). Proceedings. 2000 IEEE/RSJ International Conference on , Vol.1, 2000, Pages: 793- 798 vol.1

[7] Chanhak, C., 2001 Tiny Mobile Robots, Online: http://chanhak.com.ne.kr/robot.html/

[8] Chou, C.P.; Hannaford, B., Measurement and Modeling of McKibben Pneumatic Artificial Muscles, *Robotics and Automation,* IEEE Transactions on , Vol.12, Iss.1, 1996, Pages: 90- 102

[9] Clark, J.E.; Cham, J.G.; Bailey, S.A.; Froehlich, E.M.; Nahata, P.K.; Full, R.J.; Cutkosky, M.R., Biomimetic design and fabrication of a hexapedal running robot, *Robotics and Automation,* 2001. Proceedings 2001 ICRA. IEEE International Conference on , Vol.4, 2001, Pages: 3643- 3649 vol.4

[10] Cocatre-Zilgien, Jan Henri; Autopod 0.33, Online: http://www.fzi.de/divisions/ipt/WMC/preface/node50.html

[11] Colbrunn, R.W.; Nelson, G.M.; Quinn, R.D., Design and control of a robotic leg with braided pneumatic actuators, *Intelligent Robots and Systems,* 2001. Proceedings. 2001 IEEE/RSJ International Conference on , Vol.2, 2001, Pages: 992- 998 vol.2

[12] Drennan, B., Evolving Neural Networks for Control of a Biologically-Inspired Robot M S Thesis in works, Case Western Reserve University, Cleveland, OH, 2002

[13] Drenner, A.; Burt, I.; Dahlin, T.; Kratochvil, B.; McMillen, C.; Nelson, B.; Papanikolopoulos, N.; Rybski, P.E.; Stubbs, K.; Waletzko, D.; Yesin, K.B., *Mobility*

enhancements to the scout robot platform Robotics and Automation, 2002. Proceedings. ICRA '02. IEEE International Conference on, Vol.1, 2002, Pages: 1069- 1074

[14] Endo, G.; Hirose, S. Study on roller-walker, *Robotics and Automation,* 2000. Proceedings. ICRA '00. IEEE International Conference on , Vol.3, 2000, Pages: 2808-2814 vol.3

[15] Espenschied, K.S., Biologically-Inspired Neural Network Control of a Hexapod Robot, M.S. Thesis, Case Western Reserve University, Cleveland, OH, 1992

[16] Fukui, R.; Torii, A.; Ueda, A., Micro robot actuated by rapid deformation of piezoelectric elements *Micromechatronics and Human Science*, 2001. MHS 2001. Proceedings of 2001 International Symposium on , Vol., 2001, Pages: 117- 122

[17] Huber, F., Moore, T.E., Loher, W., Cricket Behavior and Neurobiology ed. Huber, F., Moore, T.E., Loher, W., Cornell University Press, 1989, New York, pg ix-xiii.

[18] Hustert, R., Gnatzy, W., The motor program for defensive kicking in crickets: performance and neural control, *The Journal of Experimental Biology* **198,** pg 1275-1283 (1995)

[19] Kingsely, D A Study Of The Viability Of Braided Pneumatic Actuators For Use On Walking Robots M.S. Thesis Case Western Reserve University, Cleveland, OH, 2001

[20] Klute, G.K.; Hannaford, B., Fatigue Characteristics Of McKibben Artificial Muscle Actuators, *Intelligent Robots and Systems*, 1998. Proceedings., 1998 IEEE/RSJ International Conference on , Vol.3, 1998, Pages: 1776- 1781 vol.3

[21] K-TEAM, SA HEADQUARTERS SWITZERLAND, Chemin du Vuasset, CP 111, 1028 Préverenges, SWITZERLAND

[22] Laksanacharoen, S.; Pollack, A.J.; Nelson, G.M.; Quinn, R.D.; Ritzmann, R.E., Biomechanics and simulation of cricket for microrobot design, *Robotics and Automation,* 2000. Proceedings. ICRA '00. IEEE International Conference on , Vol.2, 2000, Pages: 1088- 1094 vol.2

[23] Linzhi Sun; Yanan Zhang; Ping Sun; Zhenbang Gong, Study on robots with PZT actuator for small pipe, *Micromechatronics and Human Science*, 2001. MHS 2001. Proceedings of 2001 International Symposium on , Vol., 2001, Pages: 149- 154

[24] Muscato, G.; Guccione, S., Test of the hybrid robot WHEELEG on a volcanic environment, *Advanced Intelligent Mechatronics, 2001*. Proceedings. 2001 IEEE/ASME International Conference on , Vol.1, 2001, Pages: 3- 3

[25] Nelson, G.M., Learning About Control of Legged Locomotion Using a Hexapod Robot with Compliant Pneumatic Actuators, PhD Dissertation, Case Western Reserve University, Cleveland, OH, 2002

[26] Nelson, G.M.; Quinn, R.D.; Bachmann, R.J.; Flannigan, W.C.; Ritzmann, R.E.; Watson, J.T., Design and Simulation of a Cockroach-like Hexapod Robot, *Robotics and Automation*, 1997. Proceedings., 1997 IEEE International Conference on , Vol.2, 1997, Pages: 1106- 1111 vol.2.

[27] Osuka, K.; Kimura, T.; Ono, T., H/sup infinity / control of a certain nonlinear actuator, *Decision and Control, 1990.*, Proceedings of the 29th IEEE Conference on , 1990, Pages: 370- 371 vol.

[28] Sitti, M., PZT actuated four-bar mechanism with two flexible links for micromechanical flying insect thorax, *Robotics and Automation, 2001*. Proceedings 2001 ICRA. IEEE International Conference on , Vol.4, 2001, Pages: 3893- 3900 vol.4

[29] Shih, C.-L.; Lai, B.-K.; Kahn, H.; Phillips, S.M.; Heuer, A.H., A robust co-sputtering fabrication procedure for TiNi shape memory alloys for MEMS, *Microelectromechanical Systems, Journal of*, Vol.10, Iss.1, 2001, Pages: 69- 79.

[30] Slocum, A.C., Downey, D.C. and Beer, R.D. (2000). Further experiments in the evolution of minimally cognitive behavior: From perceiving affordances to selective attention. In J. Meyer, A. Berthoz, D. Floreano, H. Roitblat and S. Wilson (Eds.), *From Animals to Animats 6: Procceedings of the Sixth International Conference on the Simulation of Adaptive Behavior* (pp. 430-439). MIT Press.

[31] Stephen, L.K., Gosline, J.M., Ontogenetic Scaling of jump performance in the African desert locust (*schistocerca gregaria), The Journal of Experimental Biology* **177,** 81-111 (1993)

[32] Tauber E., Camhi, J.M., The wind-evoked escape behavior of the cricket *gryllus bimaculatus:* integration of behavior elements, *The Journal of Experimental Biology* **198,** pg 1895-1907 (1995)

[33] Walker, T.J., Masaki, S., Cricket Behavior and Neurobiology ed. Huber, F., Moore, T.E., Loher, W., Cornell University Press, 1989, New York, pg 1-42.

[34] Watson, J.T., Ritzmann, R.E., Pollack, A.J., Control of climbing behavior in the cockroach, Blaberus discoidalis. II. Motor activities associated with joint movement, *J Comp Physiol* A (2002) 188: 55-69